

# **Transport Processes in Orographically Induced Gravity Waves as Indicated by Atmospheric Ozone**

By  
James E. Lovill

Department of Atmospheric Science  
Colorado State University  
Fort Collins, Colorado

Prepared with support under Grant E-10-68G from the National Environmental Satellite  
Center ESSA, and from Contract AT (11-1)-1340 with the  
US Atomic Energy Commission.  
February, 1969

**Colorado  
State  
University**

**Department of  
Atmospheric Science**

Paper No. 135



TRANSPORT PROCESSES IN OROGRAPHICALLY  
INDUCED GRAVITY WAVES AS  
INDICATED BY ATMOSPHERIC OZONE

---

by  
James E. Lovill

This report was prepared with support  
under Grant E-10-68G from the  
National Environmental Satellite Center, ESSA  
and from Contract AT(11-1)-1340 with the  
U.S. Atomic Energy Commission

Department of Atmospheric Science  
Colorado State University  
Fort Collins, Colorado

February 1969

Atmospheric Science Paper Number 135

### Abstract

A high performance sailplane equipped to measure ozone, temperature and vertical velocities studied a 125 km<sup>2</sup> area simultaneous with the release of an ozonesonde and ESSA and NASA satellite observations. Theoretical Scorer parameter computations compared favorably with actual aircraft measurements. Lee wave amplitude, wavelength and vertical velocities were determined by seven independent techniques. One technique used was to measure the structure of the lee wave from an ozone implied undulating flow pattern. Another was the measurement of the wave via satellite. Unique ozone sensor flow rate calibrations were also conducted during the study.

In a second study, Boulder, Colorado, received extensive wind damage from winds greater than 56 ms<sup>-1</sup>. This occurred during large-scale descending air motions to the lee of the Continental Divide on 7 January 1969. This chinook condition is suggested to have been the result of large amplitude lee waves. Air of recent stratospheric origin is reflected in ozone concentrations at the surface in Boulder. Two mechanisms are suggested by which stratospheric air, in a short period, could arrive at the surface. Both mechanisms use as the main transport process the orographically-induced gravity wave.

## Table of Contents

	Page
List of Figures .....	v
List of Tables .....	ix
I. Introduction .....	1
Ozone theory .....	1
Lee wave theory .....	2
II. Instrumentation .....	4
Aircraft description .....	4
Ozone sensor description .....	6
Response rate .....	7
Surface equipment description. Radar .....	9
Ozonesonde .....	10
Release site .....	11
Tracking sites .....	12
Error analysis .....	12
III. Spatial Distribution of Ozone and Potential Temperature Surfaces in Orographically Induced Lee Waves .....	13
Description of flight path and area of study ....	13
Synoptic situation .....	16
Ozone and isentropic surfaces obtained from The Explorer .....	29
Computation of wavelength, amplitude and vertical velocity .....	32
Wavelength computation .....	34
Amplitude .....	41
Vertical velocities .....	41
V. Mountain-Induced Lee Waves and the 1.5 Million Dollar Destruction in Boulder, Colorado, 7 January 1969 ..	43
Synoptic pattern .....	43
Discussion of the Denver and Grand Junction sound- ings in relation to possible atmospheric conditions over Boulder on 7 and 8 January .....	48
Chinook conditions in the lee of the Front Range.	53
Boulder and Mines Peak Data .....	58

	Page
V. The Transport of Stratospheric Air to the Surface by Orographical Effects .....	61
Combined mechanisms .....	61
Single mechanism .....	63
VI. Summary .....	66
Structure of the lee wave (case study 10 October 1968 .....	66
Surface destruction and orographically-induced transport processes (case study of 7 January 1969)	66
VII. Suggestions for Future Research .....	67
Acknowledgments .....	69
References .....	70
Appendix .....	73

List of Figures

Number		Page
1.	The Explorer sailplane .....	5
2.	The Explorer instrument panel .....	5
3.	Ozone and temperature recorders on The Explorer..	6
4.	Response rate of the electrochemical concentration cell .....	9
5.	Diagram encompassing area of lee wave study ....	9
6.	The carbon-iodine ozonesonde .....	10
7.	Calibration of Komhyr ozone sensor .....	11
8.	Detailed topographical map of the Continental Divide region west of Boulder .....	12
9.	View of the sharp rise of the western slope of the Continental Divide .....	13
10.	Longs Peak .....	14
11.	Lenticular cloud over Longs Peak .....	14
12.	In wave lift .....	15
13.	Surface synoptic chart for 12 GMT, 9 October 1968	16
14.	500 mb chart for 12 GMT, 9 October 1968 .....	17
15.	Surface synoptic chart for 12 GMT, 10 October 1968	17
16.	500 mb chart for 12 GMT, 10 October 1968 .....	18
17.	Surface synoptic chart for 12 GMT, 11 October 1968	19
18.	500 mb chart for 12 GMT, 11 October 1968 .....	19
19.	Plot of Scorer parameter, potential temperature and resultant wind velocity for Grand Junction, 00 GMT, 10 October 1968 .....	20
20.	Same as Fig. 19, except for 12 GMT, 10 October 1968	20
21.	Same as Fig. 19, except for Denver, 00 GMT, 10 October 1968 .....	21

Number		Page
22.	Same as Fig. 19, except for Denver, 12 GMT, 10 October 1968 .....	22
23.	Topographic relief map of Colorado and surrounding states .....	23
24.	Mesoscale vertical time section of the thermal structure from 00 GMT, 8 October to 00 GMT, 12 October 1968 .....	24
25.	Same as Fig. 19, except for Denver, 00 GMT, 11 October 1968 .....	25
26.	Same as Fig. 19, except for Denver, 12 GMT, 11 October 1968 .....	26
27.	Ozonagram for Brainard Lake from 1813-1936 GMT, 10 October 1968 .....	27
28.	Plot of ozone mixing ratio, Scorer parameter, potential temperature and resultant wind velocity, Brainard Lake, 10 October 1968 .....	28
29.	Cross-section of ozone and potential temperature surface analysis in lee of Continental Divide, 10 October 1968 .....	29
30.	East-west cross-section of potential temperature surfaces over Colorado, 20 February 1968 .....	31
31.	East-west cross-section of isotach analysis over Colorado, 20 February 1968 .....	33
32.	Photograph taken from NASA satellite ATS III, 1527 GMT, 10 October 1968 .....	34
33.	Photograph taken from ESSA VI satellite, 1805 GMT, 10 October 1968 .....	35
34.	Photograph taken from ESSA VII satellite, 1925 GMT, 10 October 1968 .....	36
35.	Cross-section east of the Continental Divide depicting frequency of location in a given increment of The Explorer during study, based on radar data, 10 October 1968 .....	38
36.	Niwot Ridge wind data 10 and 11 October, 1968 ...	39
37.	Photograph of lee waves and other cloud forms ...	40



Number	Page
38. Photograph of destroyed home immediately after high wind conditions at Boulder .....	43
39. 500 mb isotach analysis, 12 GMT, 7 January 1969..	44
40. Same as Fig. 39, except 300 mb isotach analysis..	45
41. Same as Fig. 39, except 200 mb isotach analysis..	45
42. Surface synoptic chart for 12 GMT, 7 January 1969	46
43. Same as Fig. 39, except 300 mb isotach analysis, 12 GMT, 7 January 1969 .....	47
44. Same as Fig. 39, except 200 mb isotach analysis, 12 GMT, 8 January 1969 .....	48
45. Same as Fig. 39, except 500 mb isotach analysis, 12 GMT, 8 January 1969 .....	49
46. Surface synoptic chart for 12 GMT, 8 January 1969	49
47. Same as Fig. 19, except for Denver, 00 GMT, 7 January 1969 .....	50
48. Same as Fig. 19, except for Grand Junction, 00 GMT, 7 January 1969 .....	51
49. Same as Fig. 19, except for Denver, 12 GMT, 7 January 1969 .....	51
50. Same as Fig. 19, except for Denver, 00 GMT, 8 January 1969 .....	52
51. Same as Fig. 19, except for Grand Junction, 00 GMT, 8 January 1969 .....	53
52. Same as Fig. 19, except for Denver, 12 GMT, 8 January 1969 .....	54
53. Vorticity and stability analysis for 12 GMT, 7 January 1969 .....	54
54. Same as Fig. 53, except for 12 GMT, 7 January 1969	55
55. Temperature gradient field for Rocky Mountain and surrounding states for 21 GMT, 7 January 1969 ...	56
56. Photograph of Continental Divide and surrounding features from The Explorer at 7.6 km MSL .....	57

Number		Page
57.	Plot of wind, temperature, and pressure at Mines Peak and Berthoud Pass, 7 and 8 January 1969 .....	58
58.	Plot of wind and temperature at Boulder, 7 and 8 January 1969 .....	59
59.	Mesoscale vertical time section of the thermal structure at Denver from 00 GMT, 7 January to 12 GMT, 8 January 1969 .....	62
60.	Mesoscale vertical time section of the Scorer parameter at Denver from 00 GMT, 7 January to 12 GMT, 8 January 1969 .....	64
61.	Plot of ozone density at the surface at Boulder, 00 GMT, 7 January to 04 GMT, 8 January 1969 .....	65
A1.	Wave cloud formation taken from The Explorer at 6.1 km .....	74
A2.	Rotor cloud near Longs Peak, 10 October 1968 ....	74
A3.	Multi-layer lenticular cloud near Longs Peak, fall 1968 .....	75
A4.	Multi-layer lenticular cloud near Hagues Peak, fall 1968 .....	75
A5.	Lee wave over Continental Divide as seen from Estes Park, fall 1968 .....	76
A6.	Mosaic photograph of train of six lee waves taken from The Explorer at 6.1 km MSL .....	76
A7a.	Billow cloud formations near Continental Divide, January 1969 .....	77
A7b.	As Fig. A7a, except 200mm lens .....	77
A7c.	As Fig. A7a, except 400mm lens .....	77
A8a.	Wave cloud formation to the lee of the Continental Divide, near Longs Peak, January 1969 .....	78
A8b.	As Fig. A8a, except 400mm lens .....	78

List of Tables

Number		Page
1.	Flow rate under various aircraft maneuvers .....	8
2.	Magnitude of wavelength, amplitude and vertical velocity as determined by various techniques ....	42

---



## I. Introduction

A case study was conducted during lee-waving conditions in the Colorado Rockies on 10 October 1968. An aircraft was used to probe the area using various sensors. Ozone and radiosondes were released from near the Continental Divide and at Denver. The aircraft was radar tracked for exact positioning. Additional temperature and wind data was ascertained from permanent stations at the Continental Divide. A brief case study is presented of a high surface wind situation and a probe conducted into its possible cause.

*Ozone theory.* Trace gases (artificial and natural) have been used extensively during the last two decades to better ascertain large scale atmospheric motions [e.g., Junge and Manson, 1961; Newell, 1963; Reiter, 1963a; Hering, 1966; Kruger and Miller, 1966; Machta, 1966; Breiland, 1968] and in the last decade at an ever increasing tempo to measure smaller scale atmospheric flows, e.g., pollution in urban areas and upper and lower troposphere motions [Newell et al., 1966].

A trace gas recognized for its quasi-conservative properties at certain altitudes and in certain regions of the atmosphere is tri-atomic oxygen or ozone. In the region of the troposphere and the lower stratosphere, due to the property of recombination, ozone can generally be considered a quasi-conservative entity [Paetzold, 1953].

Regener [1941] first advanced the theory that ozone in the troposphere originated in the stratosphere. The obvious exception to this is the ever growing ozone production in the lower troposphere by urban complexes [Lea, 1968; Lovill and Miller, 1968]. The surface is generally a sink [Regener, 1957] for ozone. Of more interest in the higher atmosphere, dust and other gases can result in the destruction of ozone [Dillemuth et al., 1960; Pittock, 1966]. Dust and other material tend to concentrate at the base of temperature inversions in the troposphere and it would seem that ozone destruction would be at its maximum here rather than immediately above or below, however studies have shown that the maximum of ozone is found within the inversion--near the middle--rather than at the base [Lovill and Miller, 1968]. It is essential in tracing that one knows the source of the constituent

eing used. Near complexes that produce ozone at the surface, one must take paramount consideration of the fact that the tracer depends upon upward mixing. Above one to two kilometers one can restrict the number of sources to, in general, one--that of the stratosphere. *Kroening and Key* [1962] suggested that ozone soundings which they conducted indicated rivers of ozone flowing from the stratosphere to the troposphere. A study (centered two kilometers above and below the tropopause) indicated a possible method of transport from the stratosphere, across the tropopause, into the troposphere [*Lovill*, 1968]. By detailed observation of ozone and potential temperature, the construction of a picture regarding fine scale structure and motions is possible. The study was concerned with 21 cases at an average height of 18 kilometers and indicated that in the stratosphere were finite layers (laminae) with higher momentum, lower potential temperature, and higher ozone content than layers immediately above or below. Even more interesting was that in the upper troposphere layers were found that had lower momentum, higher potential temperature, and higher ozone concentrations than layers immediately below or above. This paper will be concerned with using these "rivers" or filaments of ozone together with its quasi-conservative property to trace atmospheric motions in the middle and upper troposphere.

*Lee wave theory.* A barrier can affect the horizontal component of air perpendicular to it in three ways: (1) that the air will be forced to rise over the obstacle, or (2) that the air will move around the barrier, or (3) a combination of one and two. If the barrier is made infinitely long perpendicular to the flow, the only possibility will be (1). In general, possibility (1) presents the best case for a wind impinging on the generally N-S-oriented Rocky Mountains. The first studies into the atmospheric flow patterns produced by mountain ranges were conducted by *Lyra* [1943] and *Queney* [1947]. *Lyra* [1943] in his theoretical treatment obtained lee waves such that the amplitude of the wave decreases downstream and increases with height. *Queney* [1947] demonstrated, among other things, that the vertical component of the earth's rotation and the amount of stability directly affected, and

contributed highly to, the wave equations developed in his theory of perturbations in stratified currents.

The solutions derived by Lyra and Queney suffered inadequacies and this was recognized by *Scorer* [1949, 1953, 1954] in different approaches to the problem. As a practical matter, it is known that the very long wavelengths discussed by Queney are not the typical lengths encountered in the lee of mountains [*Lilly*, 1968]. It is also known that the wave amplitude decreases at great heights in the atmosphere. In deriving an equation for the stream function, *Scorer* [1949] studies a case that has isentropic flow, and that is laminar, frictionless, and stationary. In addition, due to the small wavelengths involved, he neglects the earth's rotation. With these simplifying assumptions, the following equation is derived

$$\frac{\partial^2 \psi}{\partial z^2} - \left( \frac{g}{c^2} + \beta \right) \frac{\partial \psi}{\partial z} + \left( \frac{g\beta}{U^2} - \frac{1}{U} \frac{\partial^2 U}{\partial z^2} - k^2 \right) \psi = 0 \quad (1)$$

where  $\psi$  = stream function

$c^2$  = speed of sound

$\beta$  = static stability =  $\frac{1}{\theta} \frac{\partial \theta}{\partial z}$

$U$  = wind speed (generally computed normal to the mountain in the undisturbed air stream)

$z$  = height measured vertically upward

$k$  = wave number in x-direction

$\frac{\partial^2 U}{\partial z^2}$  = change of wind shear in the vertical.

In the above equation, *Scorer* neglects  $\partial \psi / \partial z$  implying that its effect is small. The equation therefore simplifies to

$$\frac{\partial^2 \psi}{\partial z^2} + \left[ \left( \frac{g\beta}{U^2} - \frac{1}{U} \frac{\partial^2 U}{\partial z^2} \right) - k^2 \right] \psi = 0 \quad (2)$$

In (2)  $\frac{g\beta}{U^2} - \frac{1}{U} \frac{\partial^2 U}{\partial z^2}$  is referred to as  $\ell^2$  and called the Scorer parameter. It is indicative of the possibility of the formation of lee waves and, out of theoretical necessity, its magnitude after being high in the lower troposphere must assume lower values at greater heights. *Scorer* showed that with two layers, the lower of depth  $h$ , a wave can occur if

$\ell^2_{\text{lower}} - \ell^2_{\text{upper}} > \frac{\pi^2}{4h^2}$ . This requirement for lee waves, in conjunction with the changes of  $\ell^2$  as a function of height, has been discussed by many researchers [Scorer, 1949; Corby, 1954; Foldvik, 1962; Conover, 1964]. The second term in the Scorer parameter (the vertical wind shear) is difficult to compute from the ordinary two-minute interpolated winds obtained during a radiosonde ascent. In addition, it is rather obvious that even a small change in the  $U$  with height results in a rather large fluctuation of the  $\partial^2 U / \partial z^2$ . (Attempts were made to compute this term, but they were rather disappointing and always subject to large error.) This study will therefore neglect the vertical wind shear term (a practice frequently done [see, e.g., Foldvik, 1962; Conover, 1964]).

Orographically-produced lee waving can serve as the origin of clear air turbulence (CAT) and can be the direct cause of transport of stratospheric air to the surface [Reiter and Hayman, 1962; Reiter, 1963a; Reiter and Mahlman, 1965; Reiter and Foltz, 1967]. CAT in the vicinity of lee waves and transport across the tropopause will be of concern in this study.

## II. Instrumentation

*Aircraft description.* The aircraft used in the lee wave study was a Schweitzer 232 high-performance sailplane--The Explorer. A sailplane was chosen for two reasons: (1) the sailplane's forward speed generally remains a constant factor; a powered aircraft, on the other hand, has a variance of speed depending on power usage as the gross weight changes. The sailplane therefore comes closer to flying a true air trajectory than any other type of aircraft--the importance of this will be clear later. (2) The response rate of the atmospheric research instruments require a slow-moving airborne platform in order to obtain the best possible results during an experimental study such as this. Later, research using these instruments can be conducted using faster airborne platforms. But for the specific aim of this study, The Explorer was deemed superior.

The Explorer (Figure 1) was purchased by the Explorers Research Corporation (ERC, Lowell Thomas, honorary chairman), a non-profit affiliate of the Explorers Club of New York. \$10,000.00 of instrumen-





Figure 1. The Explorer sailplane. Location of the temperature ensor denoted by 1. The ozone sensor intake is located on opposite ide of fuselage.

ation was installed in The Explorer with cooperation and funding by SSA, AFCRL, FAA and NASA. The instrumentation is shown and described n Figure 2. With the single exception of engine controls, the instru-ent panel is the same as in a small jet.

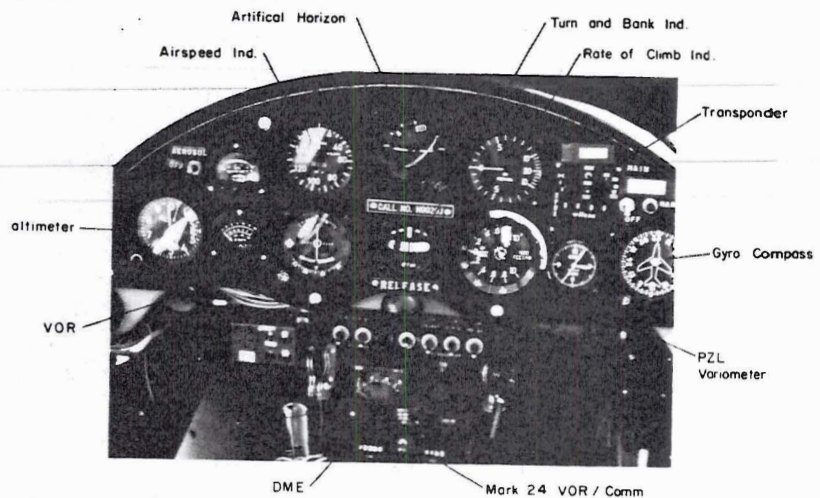


Figure 2. The Explorer instrument panel.

Physically, The Explorer can withstand 12 G's; has a glide ratio of 5:1; is equipped with oxygen for altitudes up to 45,000 feet (14 km) --with a pressure suit this could possibly be extended to 80,000 feet (25 km, 28 mb). No sailplane in the world, at this time, is equipped to perform at such high altitudes with such precision and scientific potential as The Explorer [*Pan Am Clipper*, 1968].

*Ozone sensor description.* The ozone sensor used in the aircraft was an Electro Chemical Concentration Cell (ECC) designed by *Komhyr* [1967]. The ozonesonde (a carbon-iodide (CI) ozone sensor) was of an older design [*Komhyr*, 1964; *Lovill*, 1968]. The ECC and CI ozone sensors are basically of the same internal design, response rate, size, etc. The ECC has, however, eliminated the use of carbon in the sensor system --this and other slight modifications are described by *Komhyr* [1967].

Various flow rates and sensor response are described below (the description of the sensor is elaborated upon in the section describing the CI ozonesonde). The ozone sensor recording device was mounted in front of the meteorological observer positioned in the rear seat (Figure 3).

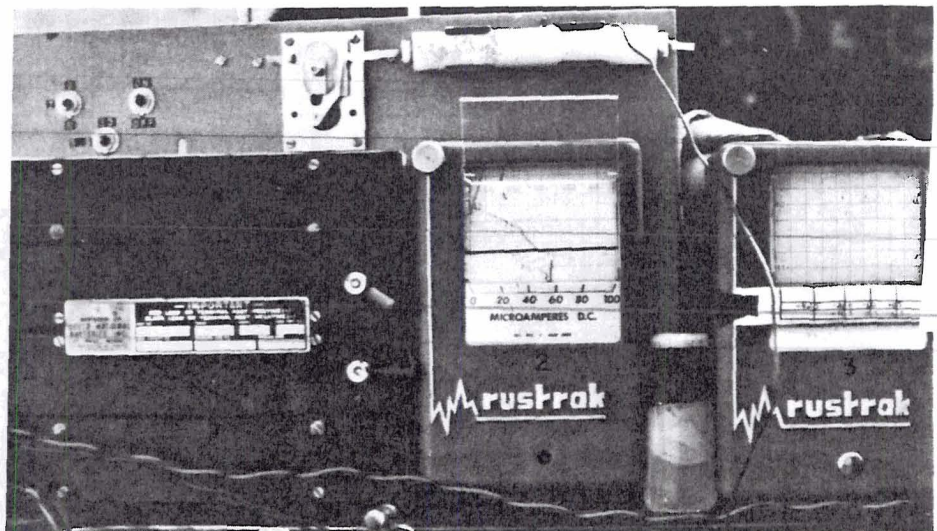


Figure 3. Ozone and temperature recorders on The Explorer. The display is situated for viewing by the meteorological observer in the rear compartment. (From left to right: 1 - ozone sensor battery, 2 - ozone sensor recorder, 3 - temperature sensor recorder.) Note instrument panel is visible in the background.

This positioning allowed the observer to have clear viewing access of the ozone sensor recording chart and the temperature probe chart (Figure 3, location 2 and 3, respectively), in addition to the control panel in front of the pilot. The Explorer cabin is not heated, and since it is important for the general performance and response rate of the ECC sensor to maintain temperatures greater than 0°C, the sensor was placed in a stationary position within the observer's parka. The temperature of the sensor was monitored and maintained nearly constant. Space limitation prevented the use of a heating cabinet.

Before the ozone data gathering process was begun, it was deemed necessary to ascertain to what extent the flow rate of the ozone sensor could be affected by various aircraft maneuvers. The type of maneuver, altitude, vertical velocity and flow rate are presented in Table 1. This experiment indicated, interestingly, that the greatest change in air flow (extreme limits) was only 1.3%. A fraction of this could be a measurement error, but this was minimized by taking five cases for each set of data. The deviation from an average value is approximately .7%, therefore the error limit probably ranges from 0.5-1.0%. In most all studies, this is well within the required accuracy of the experiment. For the purposes of this study, the error was considered negligible.

*Response rate.* The electrochemical sensor, while measuring ozone on an absolute scale, does not have an instantaneous response time. The response time of the sensor used is indicated (Figure 4) from laboratory tests made immediately prior to the flight. The experiment was conducted at 296°K. Indicated is a 54% step change in 10 seconds and a 97% change in 60 seconds. For the aircraft velocities of this study, the ozone sensor response was well within the tolerable lag limits.

The temperature probe consisted of a rod thermistor and self-contained recorder unit constructed at NCAR especially for the study. The location of the temperature probe in Figure 1, the ozone sensor location is positioned on the opposite side of the aircraft in the same location).

Table 1. Flow rate under various aircraft maneuvers.

Type of Maneuver*	Altitude (meters)	Average Flow Rate (ml/min)
On "tow" - ascending at $1.3 \text{ ms}^{-1}$ - airspeed $\sim 35 \text{ ms}^{-1}$ - heading $270^\circ$ .	4,850	181.8
Descending - airspeed $\sim 30 \text{ ms}^{-1}$ - heading $270^\circ$ .	4,150	180.6
Descending - airspeed $\sim 38 \text{ ms}^{-1}$ - heading $90^\circ$ .	3,660	179.6
Ascending - airspeed $\sim 28 \text{ ms}^{-1}$ - $30^\circ$ bank - heading $330^\circ$ .	3,810	181.7
Zero rate of climb - airspeed $\sim 30 \text{ ms}^{-1}$ - heading $310^\circ$ .	3,750	179.3
Side slip - airspeed $\sim 33 \text{ ms}^{-1}$ - heading $270^\circ$ .	2,530	179.5
Descending at $5.5 \text{ ms}^{-1}$ - airspeed $\sim 50 \text{ ms}^{-1}$ - heading $90^\circ$ .	2,780	179.6

\* wind at 4,570 meters =  
 $270^\circ$  at  $\sim 15 \text{ ms}^{-1}$ .

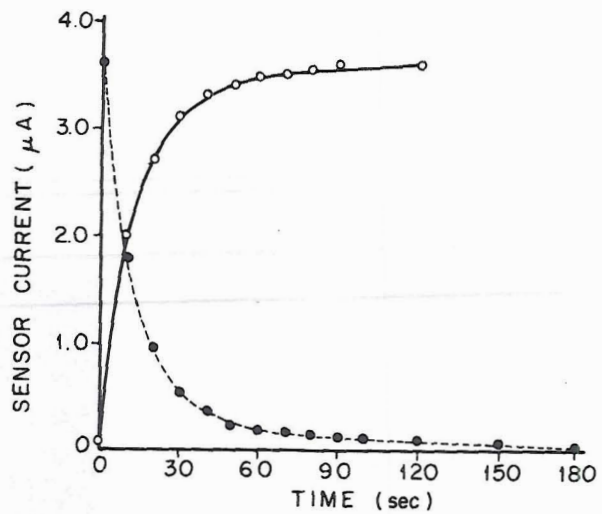


Figure 4. Response rate of the electrochemical concentration cell (Komhyr Ozone Sensor). See text for elaboration.

*Surface equipment description. Radar.* The positioning of the aircraft was obtained by an NCAR automatic radar tracking system (modified T33) (see Figure 5 for location of the unit). The accuracy of the system at 38 kilometers is  $\pm 14$  meters. Exact x, y, z location was therefore obtained continuously.

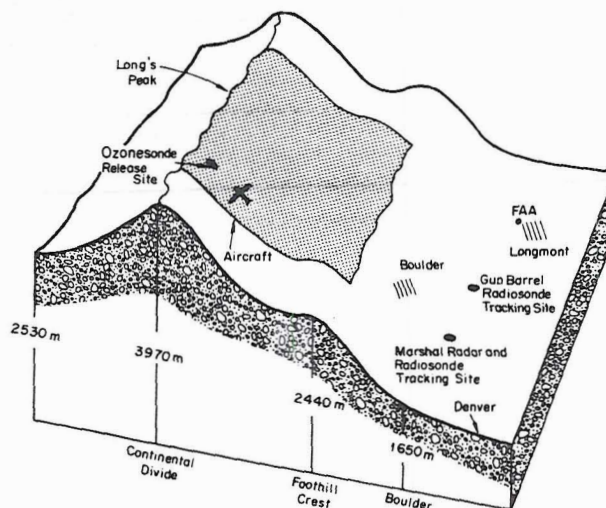


Figure 5. Diagram encompassing area of lee wave study.

*Ozonesonde.* A carbon iodide (Komhyr) ozonesonde was used in the study (Figure 6). The device was chosen because of several attributes: it is simple in design, lightweight, compact, and capable of providing data on an absolute scale. This device has been extensively described by Komhyr [1964, 1968] and used successfully in a study in California [Lovill and Miller, 1968].

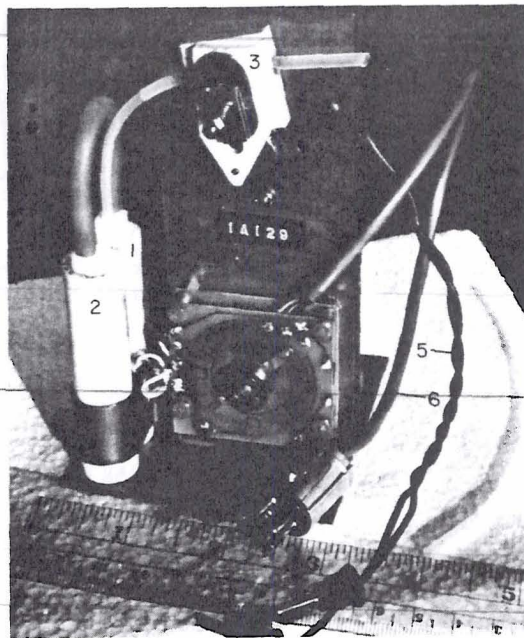


Figure 6. The carbon-iodine ozonesonde (the earlier model of the Komhyr ECC ozone sensor). Denoted in the figure: 1 - cathode chamber, 2 - anode chamber, 3 - sensor pump, 4 - instrument commutator, 5 - power supply connection, 6 - channel for data flow to radiosonde transmitter.

The sensor anode and cathode, tubing and pump are constructed of Teflon, a substance inert to ozone. The CI ozone sensor in the ozonesonde required a period of one to two hours of preflight calibration several days prior to the flight. Immediately before the flight a final calibration and check was conducted (Figure 7, the sensor is receiving a high concentration of ozone from a Regener generator). The Komhyr

ozone sensor with dimensions of 13 by 8 by 7.6 cm proved most acceptable in the small space available on the aircraft.

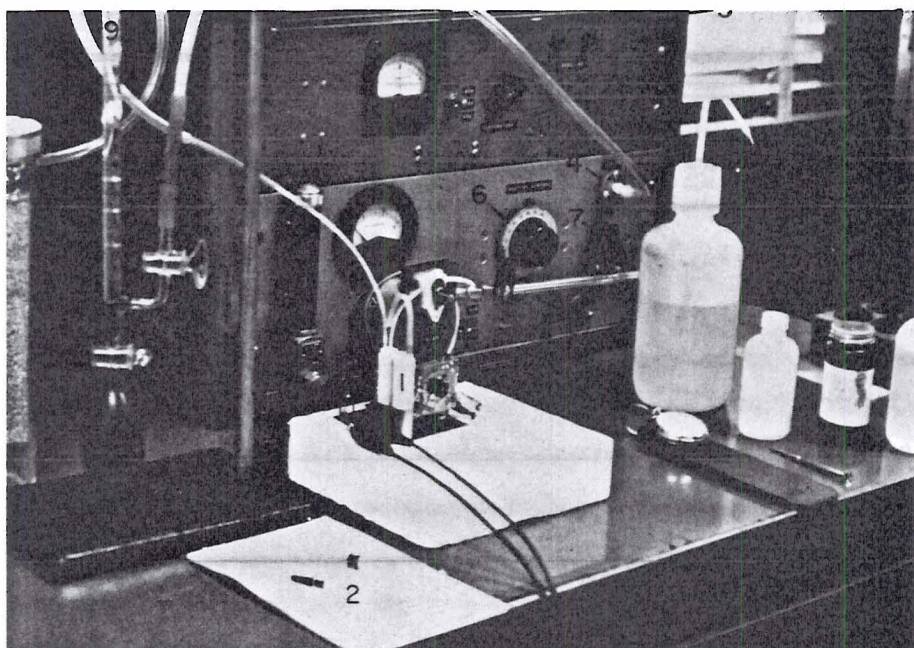


Figure 7. Calibration of Komhyr ozone sensor. Figures denote: 1 - ozone sensor, 2 - syringe and needle for solution injection into cathode and anode chambers, 3 - Regener ozone generator, 4 - air intake, 5 - air flow-rate adjustment, 6 - shutter control for ultraviolet source, 7 - ozone outlet, 8 - drying tower, 9 - flow-rate calibration buret.

*Release site.* The ozonesonde release site was selected to be Brainard Lake (BLK) which is just to the east of the Continental Divide at 3141 meters altitude (see Figures 5 and 8). The site was selected on the basis that it was easily accessible and near the Divide. It was extremely important that the ozonesonde release site be on the western boundary of the ozone lee wave tracing area (shaded area, Figure 5). One of the goals of the experiment was to attempt an aircraft rendezvous with the ozonesonde (the first time this has ever been accomplished using ozone sensors) several kilometers above and to the lee of the Brainard Lake release site. This was done in order to achieve a

comparison between the two instruments and insure a more accurate later analysis. Later analysis of the radar positioning of the aircraft and the computed ozonesonde trajectory indicated that the separation distance between the two sensors was approximately 1.3 kilometers in the horizontal.

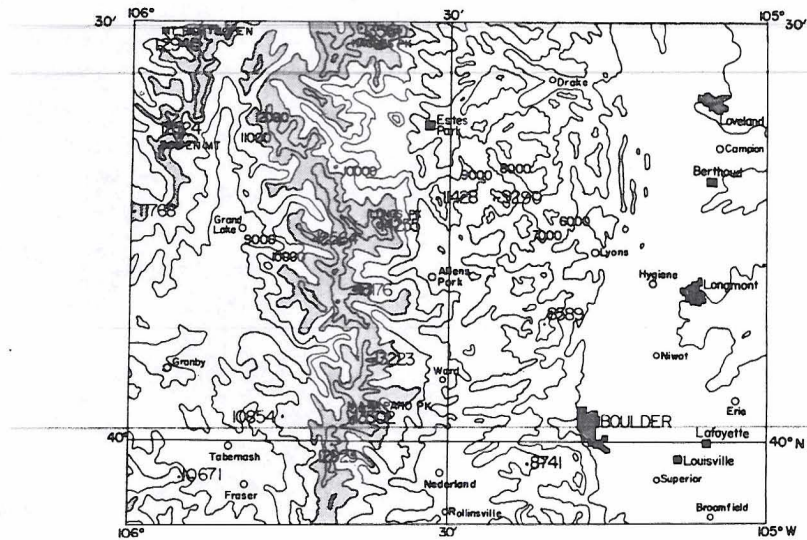


Figure 8. Detailed topographical map of Continental Divide region east of Boulder.

*Tracking sites.* The ozonesonde tracking sites were located at Marshal and Gun Barrel (see Figure 5). Two sites were provided in order to insure continuous tracking of the ozonesonde since loss of signal was possible due to the distance involved between the release site and the tracking site.

*Error analysis.* An absolute error to the 95 percent confidence limit is indicated at  $0.2^{\circ}\text{C}$  for the temperature measured by the aircraft. The probable error in an ozone data point obtained by the aircraft is less than  $\pm 5$  percent and most likely  $\pm 2$  percent. While this is to a certain extent subjective, it is none the less objective to the extent that the ozonesonde compared to  $-11\%$  with the Dobson Spectrophotometer data and all ozone data points on both sensors were corrected from this base value.



### III. Spatial Distribution of Ozone and Potential Temperature Surfaces in Orographically Induced Lee Waves

*Description of flight path and area of study.* The area of study (shaded area, Figure 5) extended (N-S) from a few kilometers north of Longmont to a few kilometers south of Boulder and (N-E) from the Front Range (Continental Divide) to just west of Boulder. Data gathering was confined to a smaller area within the above region. Figure 9 is a view of the sharp rise of the western slope of the Front Range. A powerful blocking action is forced upon a given air parcel by this steep N-S barrier.

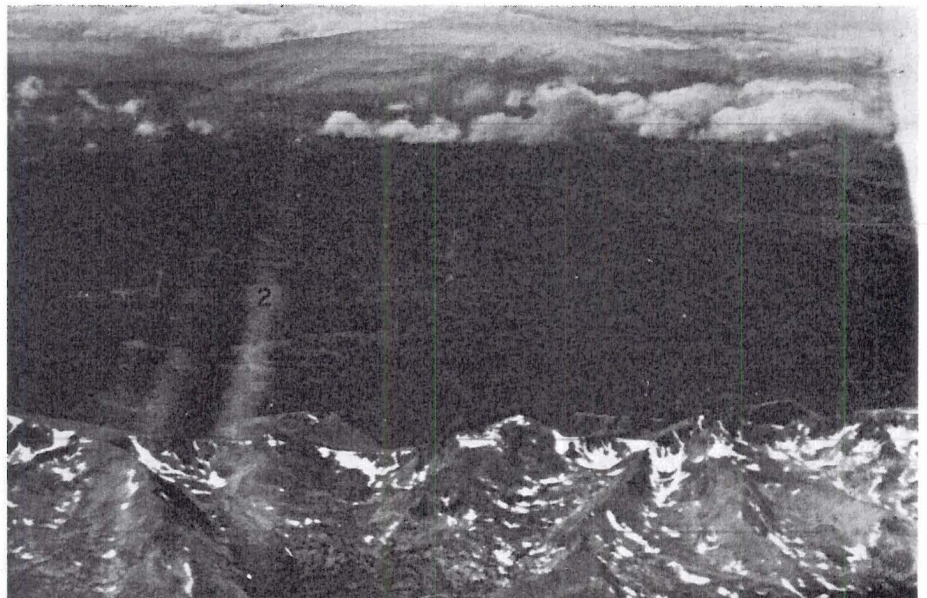


Figure 9. View (looking west) of the sharp rise of the western slope of the Continental Divide (from The Explorer at 7.6 km (25,000 feet) MSL). Denoted in figure: 1 - Continental Divide (elevation 3.9-4.3 km (12,700-14,200 feet)), 2 - Middle Park area (elevation 2.5 km (8,300 feet)).

Longs Peak (Figure 10) was the highest barrier to a given particle in the investigation area. It is not at all uncommon for a single



Figure 10. Longs Peak (as viewed from The Explorer at 6.1 km (20,000 feet) MSL). Note the extremely sharp rise of the slope.

enticular cloud (Figure 11) to form over Longs Peak even when no visible evidence of a lee wave exists elsewhere along the Front Range.

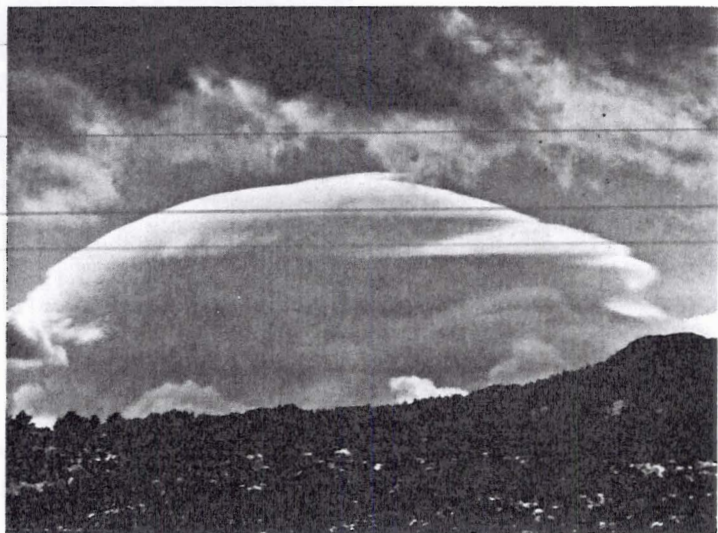


Figure 11. Lenticular over Longs Peak.

Due to its shape (Figure 10, also see topography depiction in Figure 8) and to the fact that it is situated to the east of a general N-S line of the Front Range, even low wind velocities tend to set up the mechanism producing a wave. Figure 11, in fact, was observed with a 5-6 km wind at Denver of 13 mps. Figure 12 shows The Explorer on 10 October in a wave, outside of the wave cloud itself, ascending at approximately  $10 \text{ ms}^{-1}$ . The flow within the wave is exceedingly smooth.

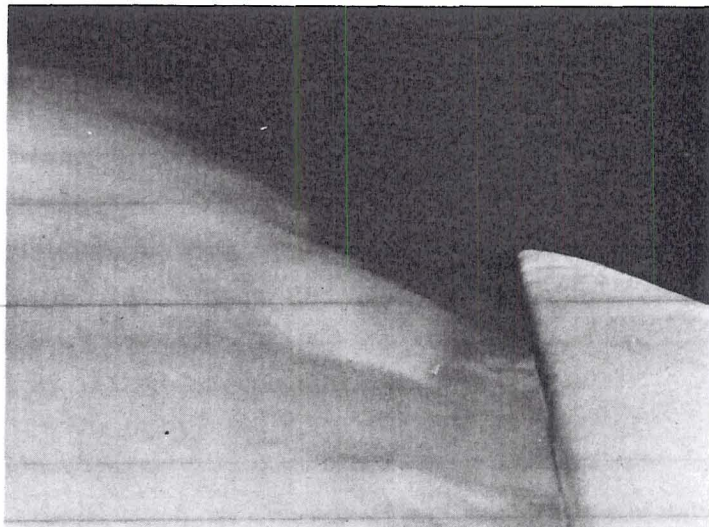


Figure 12. In wave lift. Taken from The Explorer at 5.5 km (18,000 feet) MSL, measured vertical velocity greater than  $10 \text{ ms}^{-1}$ .

No data gathering was attempted inside wave clouds although it is quite feasible as long as radar tracking is provided and the experimental area is not in a busy air traffic control area. The Longs Peak area is a busy air center and all flying above 7.32 km (24,000 feet) was radar tracked and radio controlled by the FAA Denver Center located NW of Longmont.

Turbulence was encountered on occasion near rotors in the eastern area of the region of study (see Figure 5). Although the turbulence lasted for generally less than a minute, the acceleration exceeded  $1 \text{ G}$  on occasion. Turbulence was infrequently encountered mainly due to the

act that the pilot of The Explorer was experienced in mountain wave flying. This is not always the situation, and the average pilot of a light to medium weight aircraft, if not aware, could exceed its maximum gust load.

Almost without exception, the N-S and E-W flight legs through the volume studied resulted in extremely smooth flying conditions. Flying in both the ascending and descending position of the lee waves was quite smooth and the flow seemingly laminar.

*Synoptic situation.* On 9 October (Figure 13), the Great Basin, the Rockies and most of the Great Plains were under the influence of a large anticyclonic cell. (Immediately prior to this period (36 hours) a complex frontal system had crossed the Colorado Rockies.) At 500 mb on 9 October (Figure 14), winds were W to NW at  $25 \text{ ms}^{-1}$ .

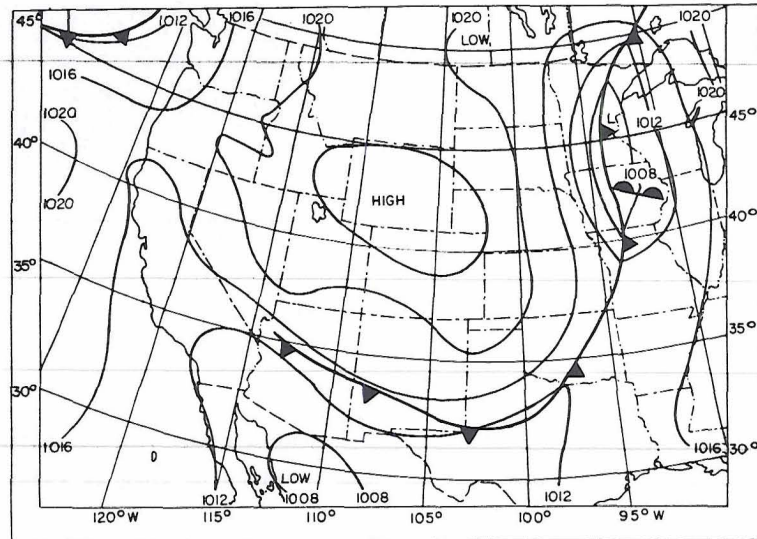


Figure 13. Surface synoptic chart for 12 GMT, 9 October 1968 (from ESSA).

At the surface on 10 and 11 October (Figures 15 and 17), a slow migration eastward of the large anticyclone, together with formation of a weak low in eastern Colorado, produced a surface wind system that

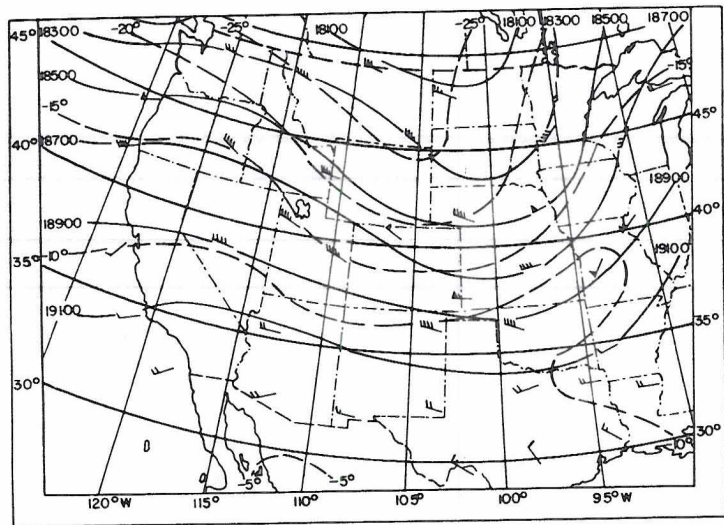


Figure 14. 500 mb chart for 12 GMT, 9 October 1968 (from ESSA).

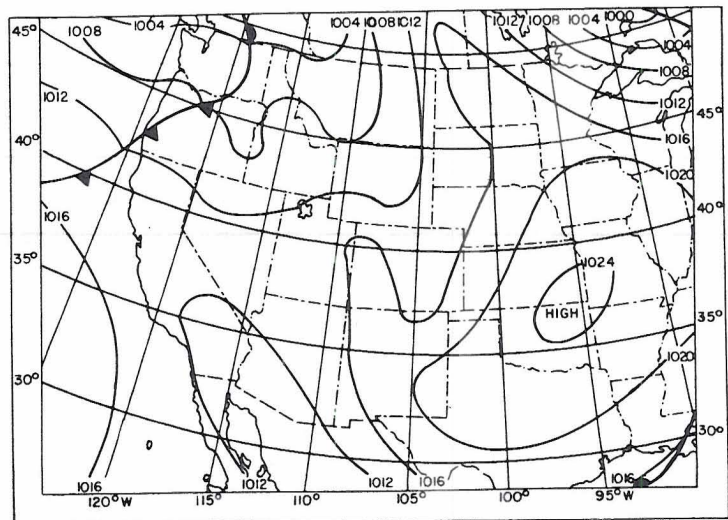


Figure 15. Surface synoptic chart for 12 GMT, 10 October 1968 (from ESSA).

resulted in generally SW surface winds of  $5 \text{ ms}^{-1}$ . At 500 mb (Figures 16 and 18) by the 11th, the flow was generally zonal throughout the western United States with velocities of  $15 \text{ ms}^{-1}$  from the WSW over most of Colorado. A short-wave pattern seemed to be exhibited in the temperature structure over NW Colorado.

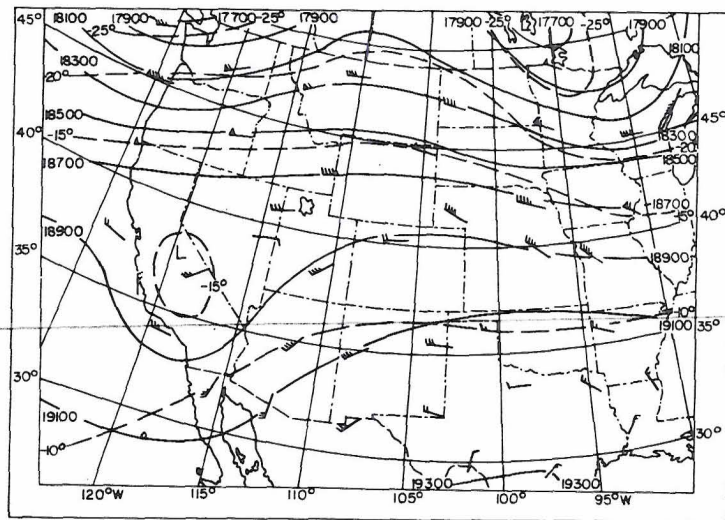


Figure 16. 500 mb chart for 12 GMT, 10 October 1968 (from ESSA).

A cursory examination on the 10th at 00 and 12 GMT (Figures 19 and 20) of the Grand Junction soundings (upstream of the area of lee wave study), indicates a wind field above 400 mb very similar to that of Denver during the same period (Figures 21 and 22). The stable layer in evidence from 310 to 300 mb at Grand Junction at 00 GMT (Figure 19) seems to have been replaced by an adiabatic layer twelve hours later (Figure 20).

In addition to the potential temperature and the resultant wind, a third parameter,  $\frac{g\beta}{U^2}$ , was obtained. The assumption was made as explained earlier that  $\frac{1}{U} \frac{\partial^2 U}{\partial z^2}$  would be neglected. In this form,  $\frac{g\beta}{U^2}$  can be referred to as the Lyra or Scorer parameter ( $\ell^2$ ). A feature noted

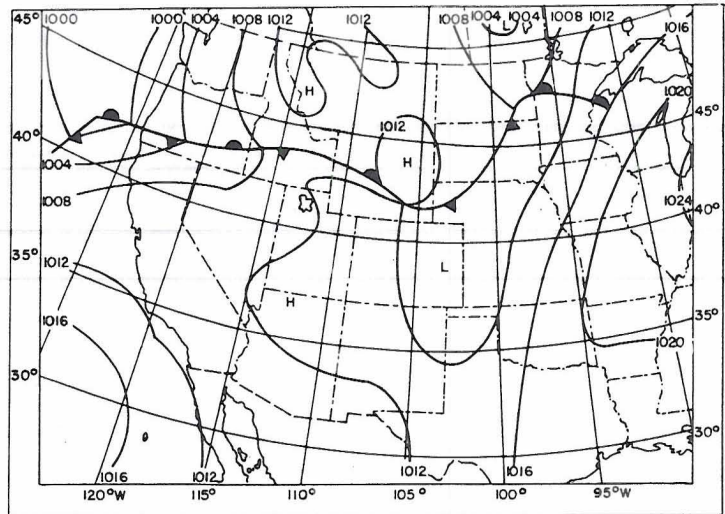


Figure 17. Surface synoptic chart for 12 GMT, 11 October 1968 (from ESSA).

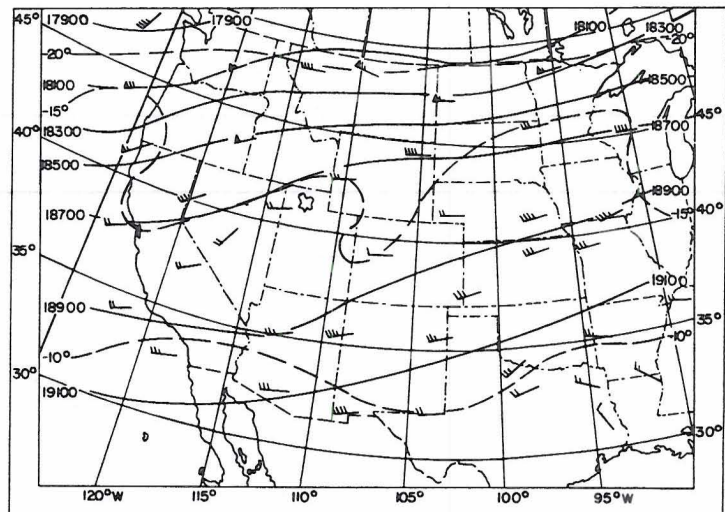


Figure 18. 500 mb chart for 12 GMT, 11 October 1968 (from ESSA).

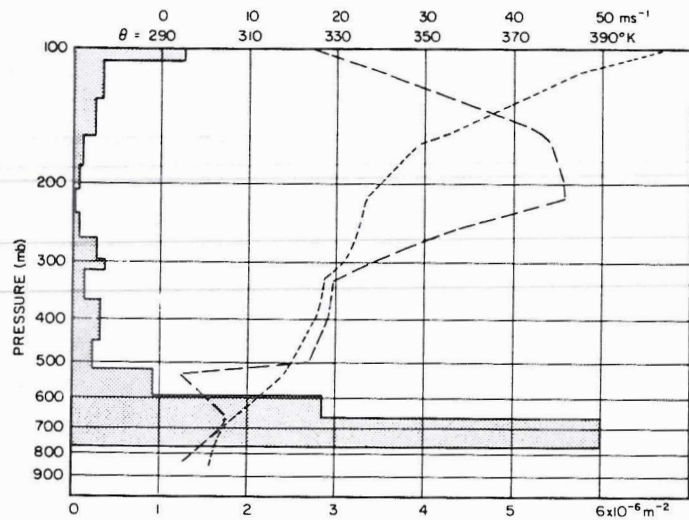


Figure 19. Plot of Scorer parameter (shaded area), potential temperature (short, dashed line), and resultant wind velocity (long, dashed line) for Grand Junction, 00 GMT, 10 October 1968.

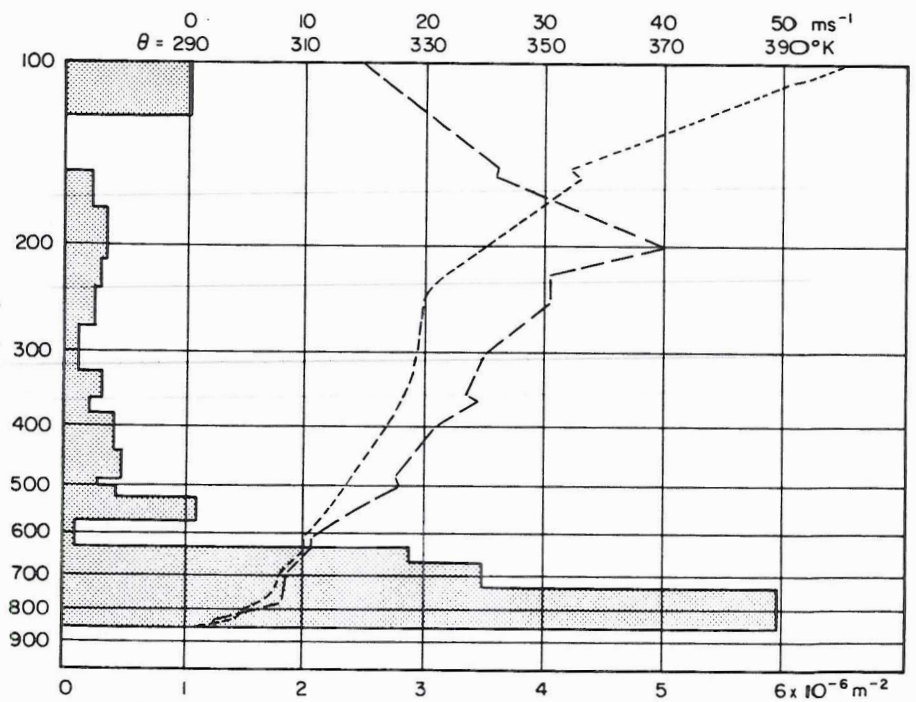


Figure 20. Same as Fig. 19, except for 12 GMT, 10 October 1968.



generally when lee waves are observed is a decrease of magnitude of  $\ell^2$  with increasing height in the troposphere. Inspection shows that this is mainly due to wind speed. There is an increase in  $\ell^2$  above the tropospheric wind maximum because of the greater stability of the stratosphere and a decrease of wind velocity [Foldevik, 1962; Scorer, 1949, 1953, 1954]. Generally required of the  $\ell^2$  profile is a large value in the lower troposphere. When  $\ell^2$  decreases by approximately an order of magnitude through a thick layer from its value at the bottom of the layer, Scorer found that only then would waves be possible.

It therefore appears (Figures 19 and 20) that atmospheric conditions were possible for wave formation at Grand Junction, however wind components and mountain alignment prohibited this apparently. However, to the lee of the Front Range (280 km west of Grand Junction), Denver and Brainard Lake soundings indicated possible lee wave formation. The possibility was verified by wave clouds. Figure 23 indicates both the topographic relief of the Rocky Mountain area in and immediately surrounding Colorado and the location of Brainard Lake relative to Grand Junction and Denver.

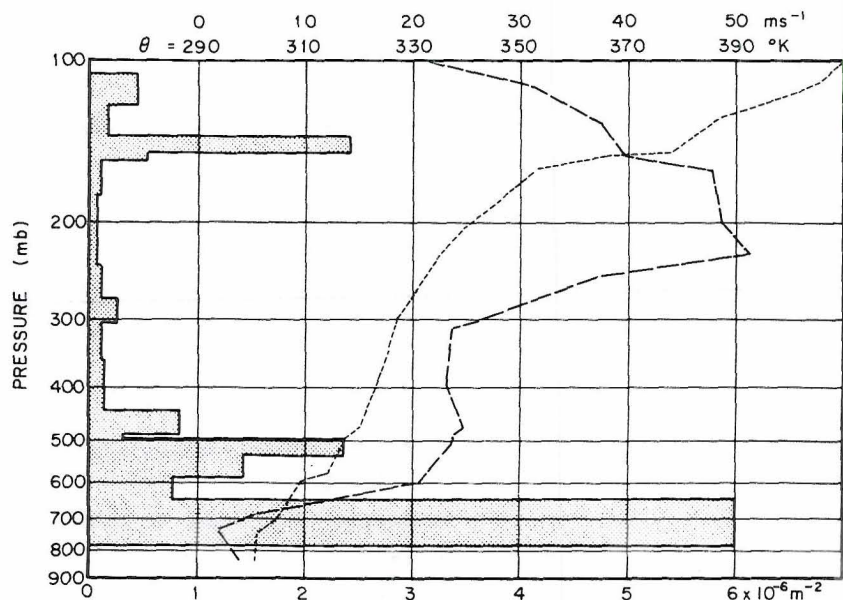


Figure 21. Same as Fig. 19, except for Denver, 00 GMT, 10 October 8.

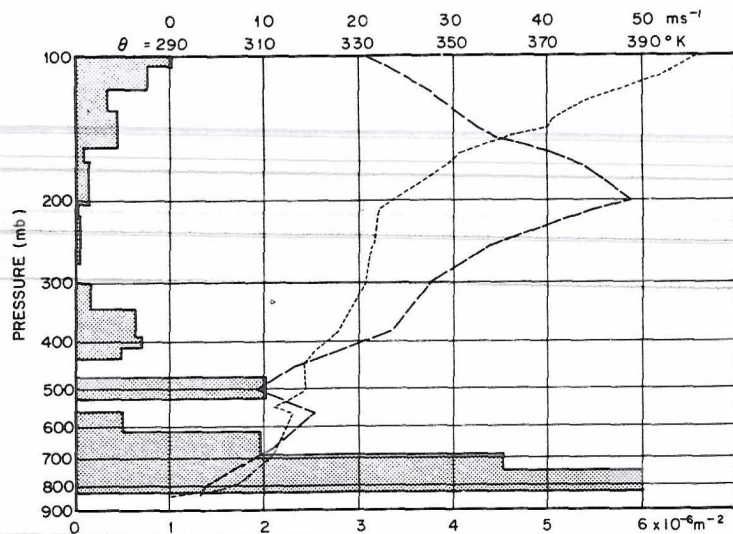


Figure 22. Same as Fig. 19, except for Denver, 12 GMT, 10 October 1968.

Analysis of soundings of Grand Junction to determine upstream conditions of the Continental Divide indicated little could be learned of lee wave formation in the lee of the Front Range that couldn't be obtained from the Denver sounding. Analysis concerning Grand Junction will be used only as peripheral evidence.

The data gathering portion of The Explorer flight on 10 October lasted from 1344 to 1955 GMT, various problems restricted the use of all of the data however. The data that were used encompass a period from 1700 to 1955 GMT. Most of the data were gathered between 400-600 mb. Therefore a past history and location of air particles in that region at the time will be analyzed using a mesoscale analysis of the Denver potential temperature and wind (Figure 24).

Air particles at the top of the area of investigation (400 mb) are indicated (Figure 24) to have been some 60 hours earlier at 260 mb. Particles arriving at 400 mb at 1830 GMT were sufficiently close to the tropopause earlier to have received higher ozone concentrations than usual for the 400-600 mb level. Particles arriving at the 600 mb level originated earlier at 480 mb. In general, air arriving at the region

of concentrated investigation--the 200 mb layer from 600-400 mb--had been subsiding for the past two days. The wind, in general, backed and decreased in velocity for a 36-hour period prior to, and during, the radiosonde sounding at Denver.

The vertical  $\lambda^2$  profile indicated lee wave formation possible on the 10th at 00 GMT (Figure 21) and indeed, as indicated, lee waves were visible during this period. The  $\lambda^2$  profile 12 hours later (Figure 22) indicated even better lee wave formation to be possible. Around this period--10 October at 12 GMT--indeed visible lee wave activity seemed most intense. According to the Denver  $\lambda^2$  profiles, the formation of lee waves was less likely at 00 GMT on 11 October (Figure 25), and even less likely twelve hours later (Figure 26). The flight period appears to have taken place during an optimum time, although the Denver profiles indicate the data sampling period missed the optimum formation (Figure 22)--being a few hours late. Under weak westerly flow conditions, when lee waving of light to moderate intensity is occurring, the strongest waving occurs during the early morning hours before convective activity has the opportunity to disrupt the wave flow.

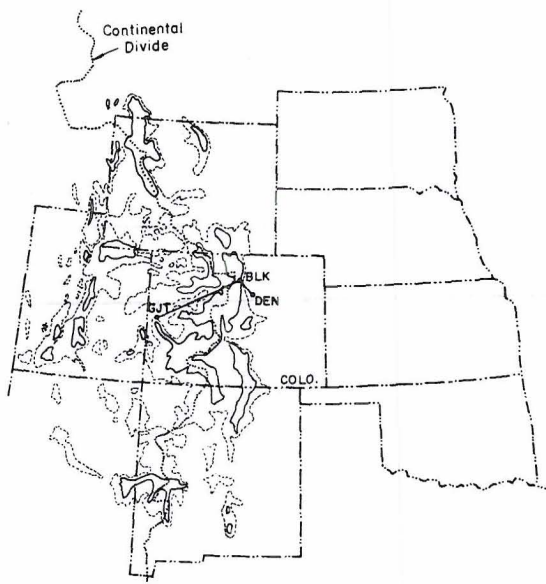


Figure 23. Topographic relief map of Colorado and surrounding states. (GJT = Grand Junction, BLK = Brainard Lake, and DEN = Denver).

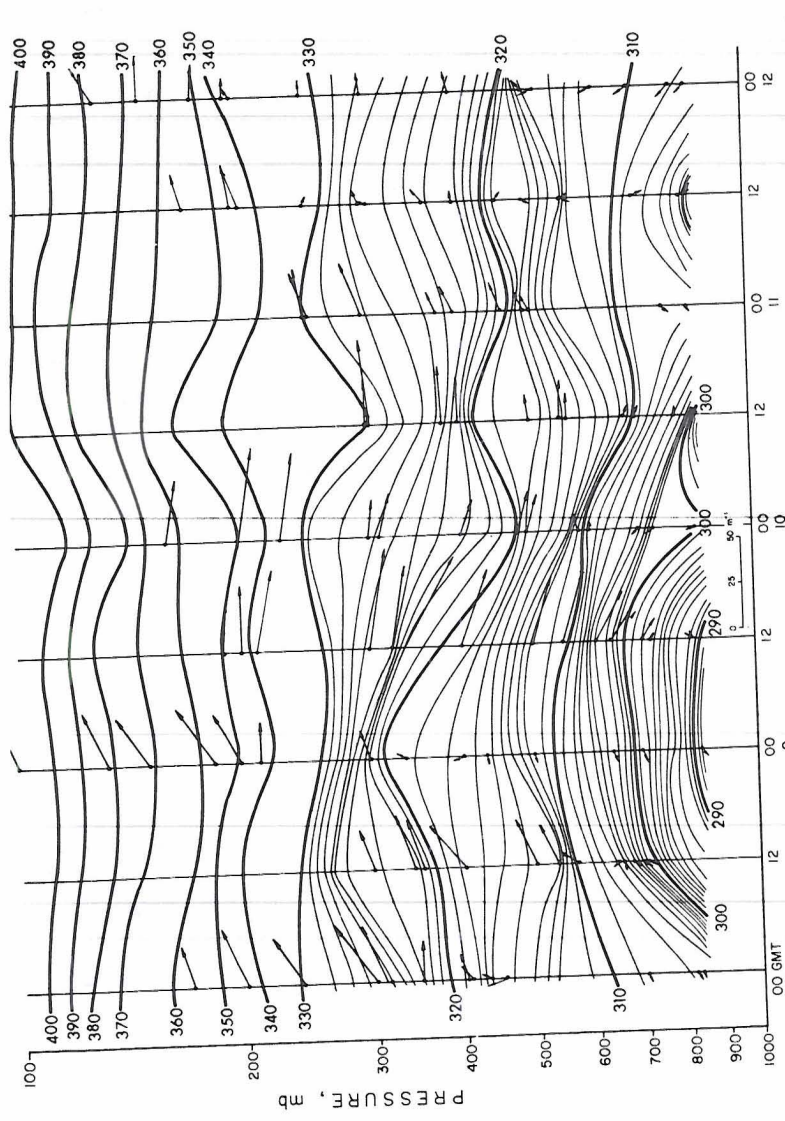


Figure 24. Mesoscale vertical time section of the thermal structure from 00 GMT, 8 October to 00 GMT, 12 October 1968 (wind vectors also plotted).

Two factors, strong wind shears and stable layers, are conducive to gravity wave formation. The Denver sounding on 10 October at 12 GMT (Figure 22) indicates a strong wind shear zone from 380-450 mb. A stable layer is indicated in this region. On 11 October at 00 GMT (Figure 25), the only strong wind shear in the region of investigation is between 550 and 600 mb. This corresponds to a nearly adiabatic layer. A stable layer is observed from 470-490 mb. The data obtained from the Brainard Lake sounding are represented by an ozonogram (Figure 7). Ozone is depicted as a function of height and partial pressure ( $\eta b$  = nanobar). From the surface to 200 mb, ozone values approximate the 70  $\eta g/g$  curve. Under nomenclature suggested previously [Lovill, 1968], this region would be denoted ozone zone number one. This is the zone in which vertical mixing is strongest through convection and turbulence.

Zone two is in evidence from 200-80 mb (12-17.5 km). It is a zone of weak ozone gradient. This is a region of change from decreasing or isobaric to increasing partial pressure (a region of increasing mixing ratio). The height of 12 km represents the ozone tropopause [Lovill,

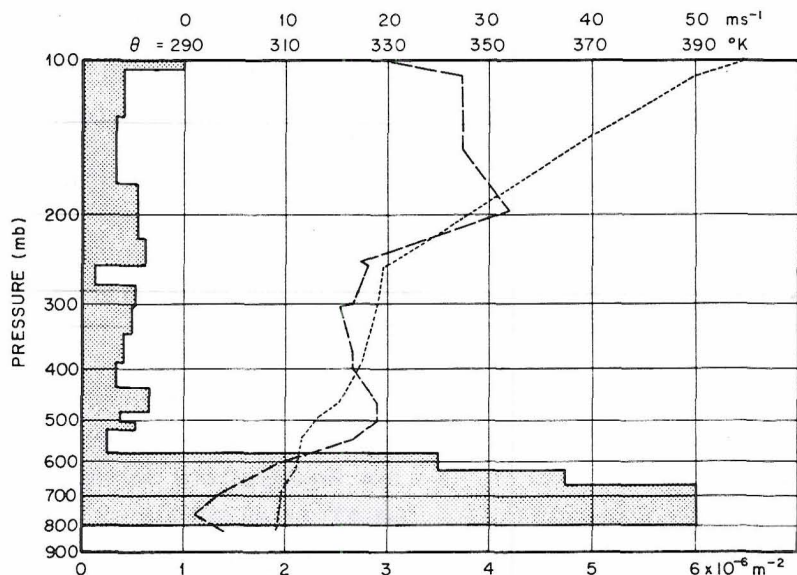


Figure 25. Same as Fig. 19, except for Denver, 00 GMT, 11 October 1968.

1968]. It is the boundary between the well-mixed tropospheric ozone and the stratospheric ozone. This zone is represented by some vertical exchange, probably in this particular case mostly through wave action.

Zone three is a layer from 80-60 mb (17.5-19.5 km). This is a zone of strong vertical ozone gradients. Ozone mixing ratios increase rapidly. Vertical exchange in this region is probably slower and is determined mainly by large-scale differential horizontal advection, and to a lesser extent by molecular diffusion.

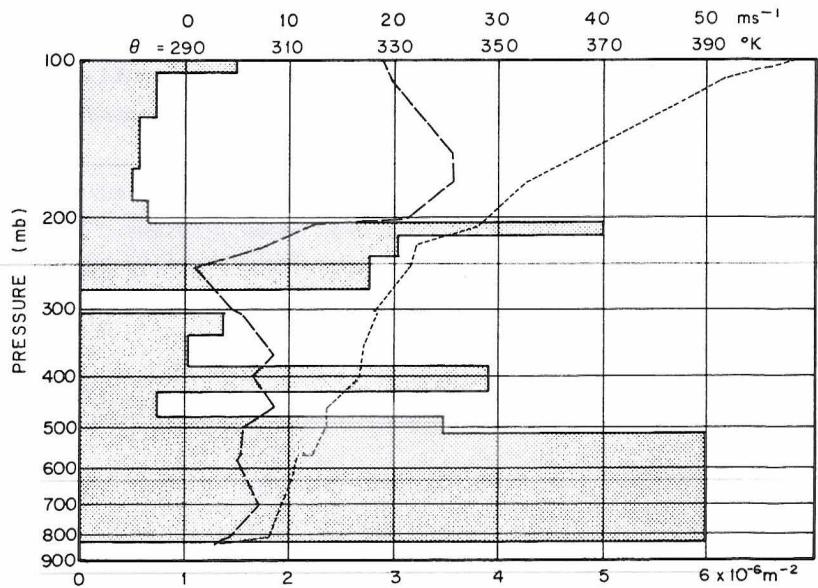


Figure 26. Same as Fig. 19, except for Denver, 12 GMT, 11 October 1968.

Zone four is representative of the region of maximum ozone production; it is also a region greatly influenced by advection. During this investigation two slight peaks are indicated of 128 nb at 52 mb and 133 nb at 26 mb.

Zone five is the region immediately above the maximum where the ozone partial pressure asymptotically approaches zero. This region represents a constant mixing ratio--in this case 10  $\mu\text{g/g}$ .

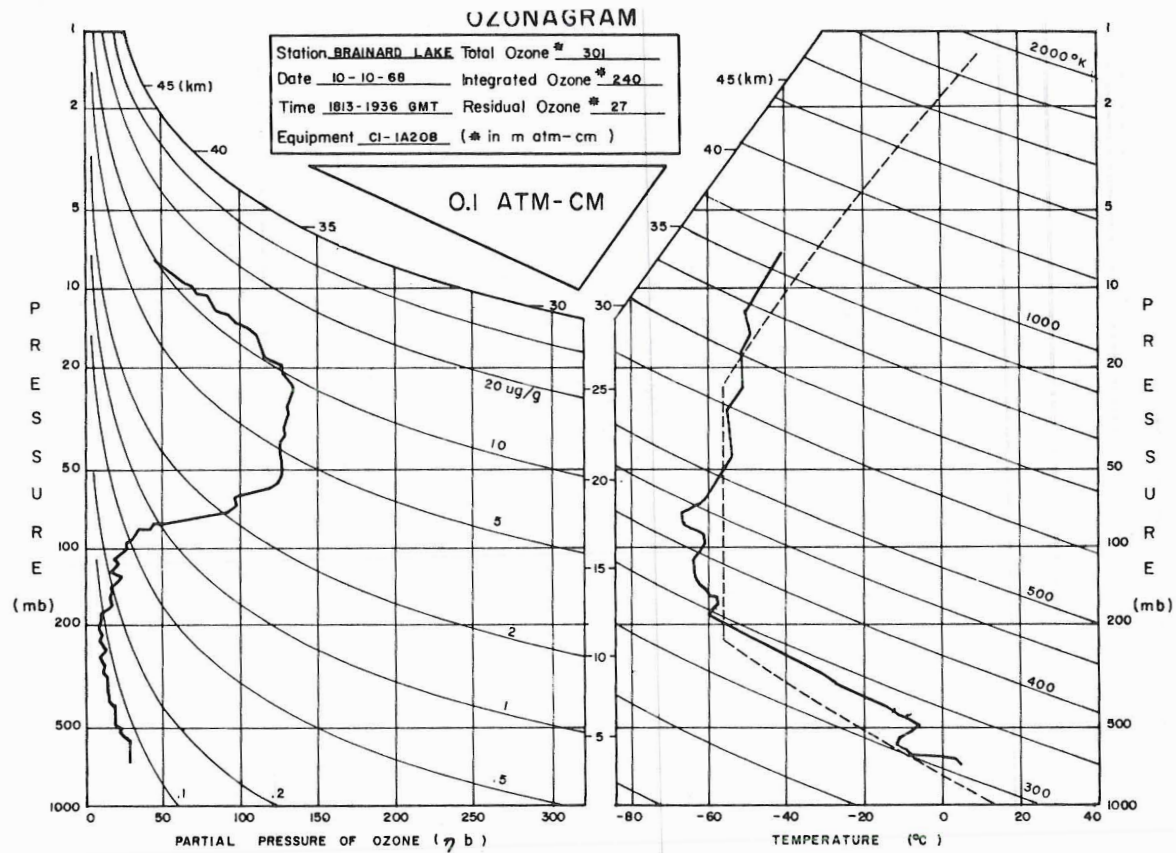


Figure 27. Ozonagram for Brainard Lake from 1813-1936 GMT, 10 October 1968.

A model has been suggested [Lovill, 1968] from which a partial explanation of the transport in the vertical of ozone (or any other atmospheric constituent) could be obtained. Vertical mixing in the vicinity of the tropopause occurring by means of wave action produces filaments of stratospheric air that are interjected into the upper troposphere. Tropospheric filaments would have high momentum, low potential temperature, and low ozone content relative to their environment; stratospheric filaments would have low momentum, high potential temperature, and high ozone content relative to their immediate environment. Mixing by eddies would tend to blur the transition zone along the edges of such laminae.

From examination of the computed Scorer parameter, potential temperature, wind velocity and ozone mixing ratio in Figure 28, several features can be noted. The surface pressure at Brainard Lake on 10 October was 690 mb. From this point to 670 mb a near adiabatic lapse rate was visible. From 670 to 650 mb, a super adiabatic layer was in evidence. Immediately above, from 650-600 mb, adiabatic conditions once again prevailed. Most interesting is the 100 mb layer from 500-600 mb.

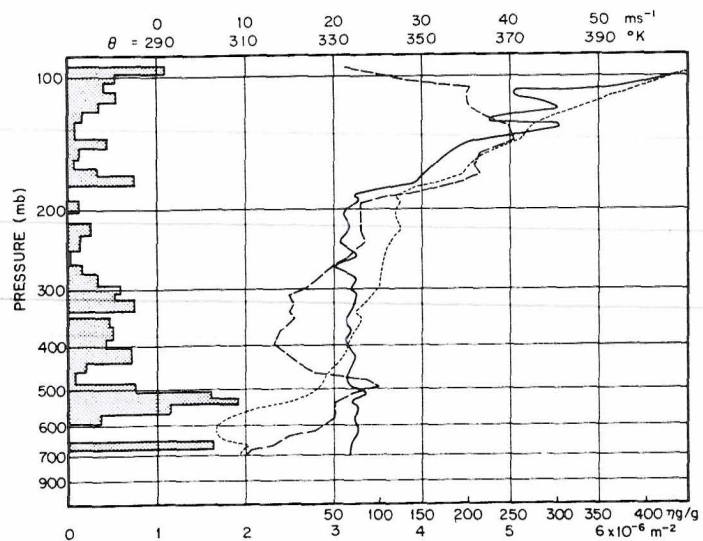


Figure 28. Plot of ozone mixing ratio (solid line), Scorer parameter (shaded area), potential temperature (short, dashed line) and resultant wind velocity (long, dashed line) at Brainard Lake, 1813 GMT, 10 October 1968.



In general, the region studied (400-600 mb) had a Scorer parameter profile indicative of possible lee wave formation, a wind jet in the center, a very stable layer in the lowest level (500-600 mb), a nearly adiabatic layer in the upper level (400-500 mb), and several ozone filaments or "tongues" throughout the layer.

*Ozone and isentropic surfaces obtained from The Explorer.* The ozone and temperature data used for the analysis of Figure 29 were obtained between a point over the ozonesonde release site at Brainard Lake and north to a point 6 kilometers from the release site (this line, N-S, is from approximately Ward to a point halfway between Ward and Allens Park; see Figure 8). East-west the data sampling area extends from the Continental Divide to 25 kilometers east of the Divide.

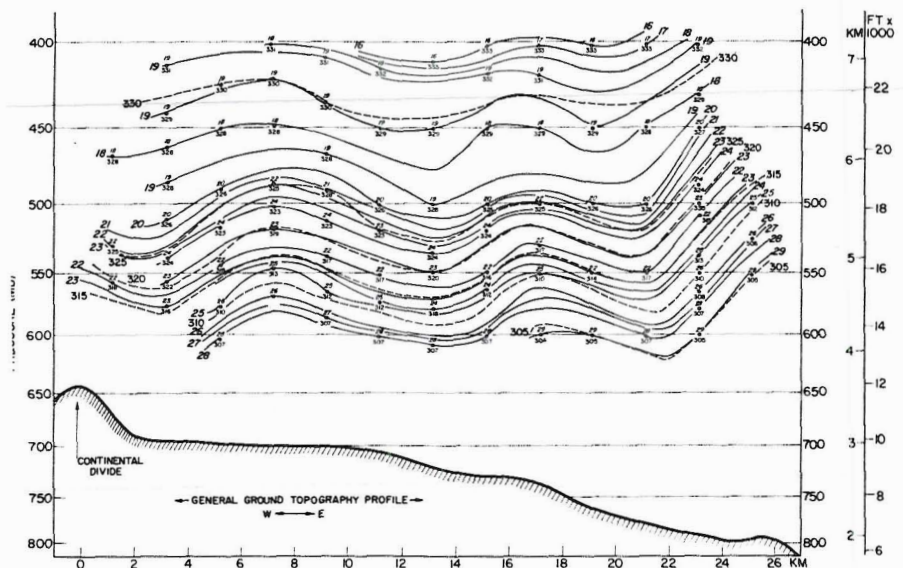


Figure 29. Cross-section of ozone (in mb partial pressure, solid line) and potential temperature (in K, dashed line) analysis in lee of Continental Divide, 10 October 1968.

The area sampled equalled  $125 \text{ km}^2$ , the volume  $375 \text{ km}^3$ . Due to the possible change in intensity of the lee wave at various positions

north and south along the Front Range, the data gathering was kept to the smallest N-S cross-section possible that still allowed acquisition of adequate data for a thorough analysis.

Examination of Figure 29 indicates several noteworthy features: (1) a waviness is exhibited in both the ozone partial pressure surfaces and the potential temperature surfaces, (2) a much steeper gradient of both parameters is seen in the lower volume (region one, 500-600 mb), (3) lines of equal ozone partial pressure (isozones) have greater spacing in the upper area (region two, 400-500 mb) than in region one.

A few ozone and temperature data points have been placed on the figure at 2 km horizontal increments and random pressure intervals. These data represent only a fraction of the data points obtained during the 175 minute period. While data sampling in the atmosphere from aircraft over a small area (125 km<sup>2</sup>) for a period of 175 minutes would usually be subject to transient effects, it is felt that this was not the case in this study. During the entire six-hour flight period, little, if any change was noticed in the physical characteristics of visible wave clouds in the region. An undercast below the wave clouds approximately 10-25 km east of the Front Range appeared to have generally dissipated near the end of the study. The lee wave is quasi-stationary with respect to a barrier and Figure 29 seems to exhibit just this (even though the sampling period was long). While the general waviness of the potential temperature and ozone surfaces don't represent streamlines, they are probably suggestive of the streamline flow.

There can be no doubt that a lee wave exists; to what extent it caused the approximate 30 mb difference in tropopause height between Brainard Lake and Denver can only be speculated upon. It is probable that the upward displacement of the tropopause at Brainard Lake is most likely the result of gravity waves. The height indicated for the tropopause at Brainard Lake is taken from a single atmospheric sounding, and the point at which the tropopause was penetrated in relation to the positioning of the wave train could perhaps mean a difference of 30 mb. This possible displacement of the tropopause is clearly seen in data collected and analyzed in the 1968 Winter Rocky Mountain Lee Wave Study (Figure 30). The wave amplitude near the tropopause in this figure is at least 30 mb.

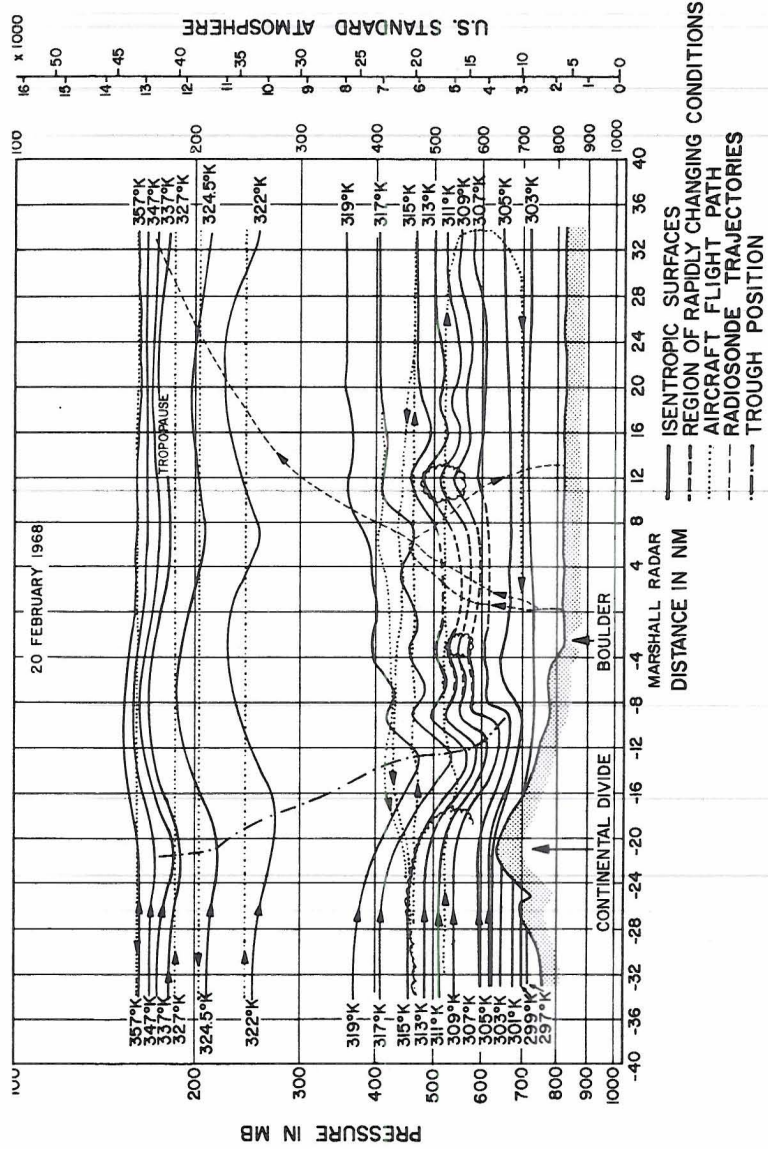


Figure 30. East-west cross-section of potential temperature surfaces over Colorado, 20 February 1968 (from winter 1968 Rocky Mountain lee wave project). (Isentropic surfaces - solid line, trough position - dot-dash line, region of rapidly changing conditions - heavy dashed line, aircraft flight paths - dot line, radiosonde trajectories - light dashed line.) (After Lilly)

A detailed wind field analysis on 10 October is not available since the aircraft was not equipped to measure horizontal wind. But the structure of the wind field during this study could be suggested from the situation on 20 February 1968 (Figure 31). The analysis of the isotachs from the several aircraft are presented here. The u-component only is analyzed. Horizontal wind speeds decrease in the main wave trough region; this is the situation up to the tropopause. The analysis of the 20 February u-component points out an interesting convergence of the wind field west of the trough at the 200 mb level and a divergence of the wind field to the lee of the trough. Just how close this wind structure was to the present case under study on 10 October is difficult to determine.

*Computation of wavelength, amplitude and vertical velocity.* The lee wave condition being studied by balloon soundings and from aircraft on 10 October was observed from satellites also by the presence of lee wave clouds. A wave system usually exists when clouds are observed to the lee of an obstacle in the airflow. As air is lifted to the wave crest, it is adiabatically cooled and moisture condenses. In this manner a wave cloud, or train of clouds, becomes visible. Clouds can be visible in the ascending region and no clouds observed in the subsiding air. Thus, if the distance between cloud trains could be measured, a wavelength could be obtained.

The lee wave conditions under study by aircraft were observed by three U.S. satellites. The NASA ATS III observed the lee wave region (Figure 32) at 1527 GMT; ESSA VI observed the lee waving at 1805 GMT (Figure 33); and ESSA VII photographed the situation at 1925 GMT (Figure 34). The data presented in this study began with a time period 65 minutes after the first satellite photograph and ended 30 minutes after the last photograph.

ATS III is positioned in an earth synchronous orbit at 22,300 mi. over the mouth of the Amazon River and photographs of western North America are therefore at the edge of the observed picture. This can easily be seen in Figure 32. A wave phenomenon appears to be in evidence in this photograph, but due to the inability to properly resolve

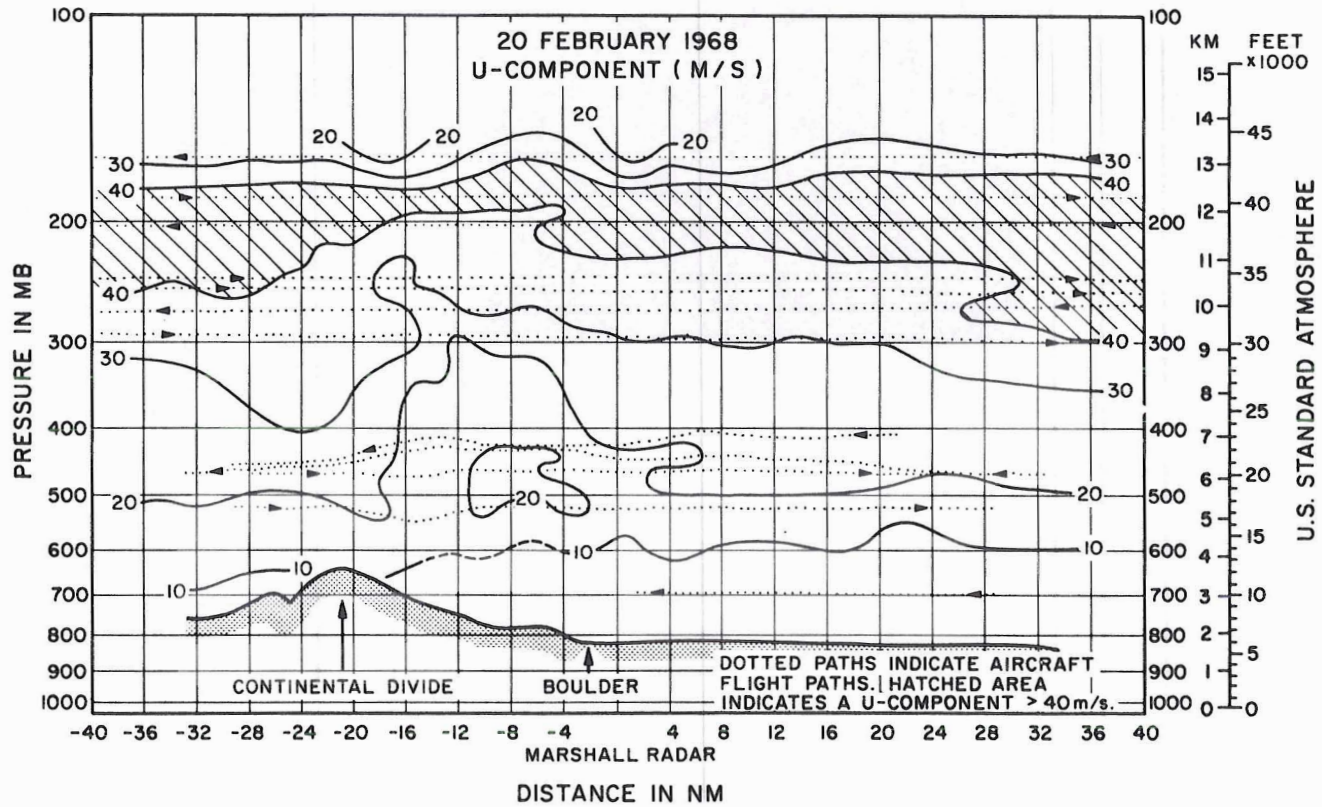


Figure 31. East-west cross-section of isotach analysis over Colorado, 20 February 1968. (Note region of minimum u-component to lee of Divide.)

the area because of the low satellite angle, computation of wavelengths will not be attempted.

ESSA VI observed the area 158 minutes later and a wave is clearly visible.

ESSA VII, 80 minutes later, photographed the same area and a wave train of four waves is now visible.

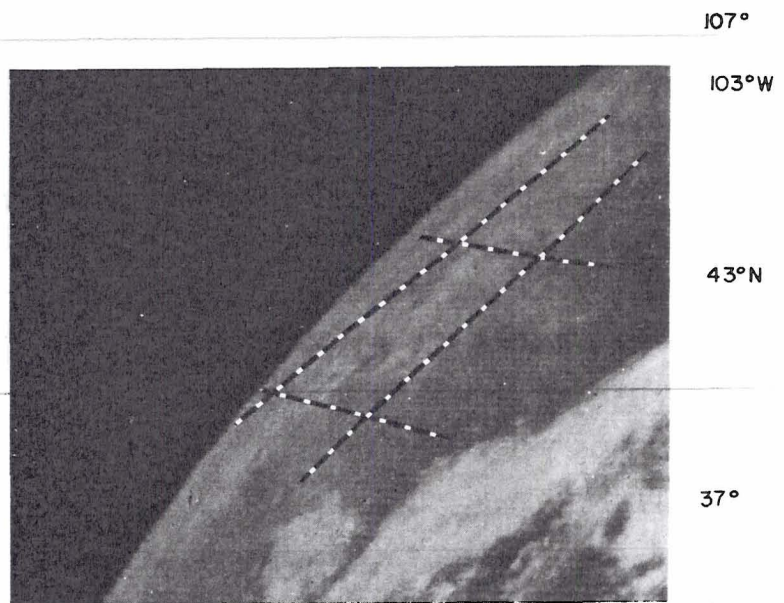


Figure 32. Photograph taken from NASA satellite ATS III, 1527 GMT, 0 October 1968.

*Wavelength computation.* From ESSA VI, a wavelength of 14.3 km was measured and from ESSA VII--13.3 km.

An examination of Figure 29 (the ozone cross-section) indicated in the lower region (500-600 mb) a wavelength of 10.0 and in the upper region a wavelength of 10.5 km. The shortest wavelength measured was 3.5 km. The potential temperature surfaces indicated a somewhat similar wavelength.

As indicated earlier, The Explorer was continuously tracked by radar to obtain exact positioning. Figure 35 depicts the percent of

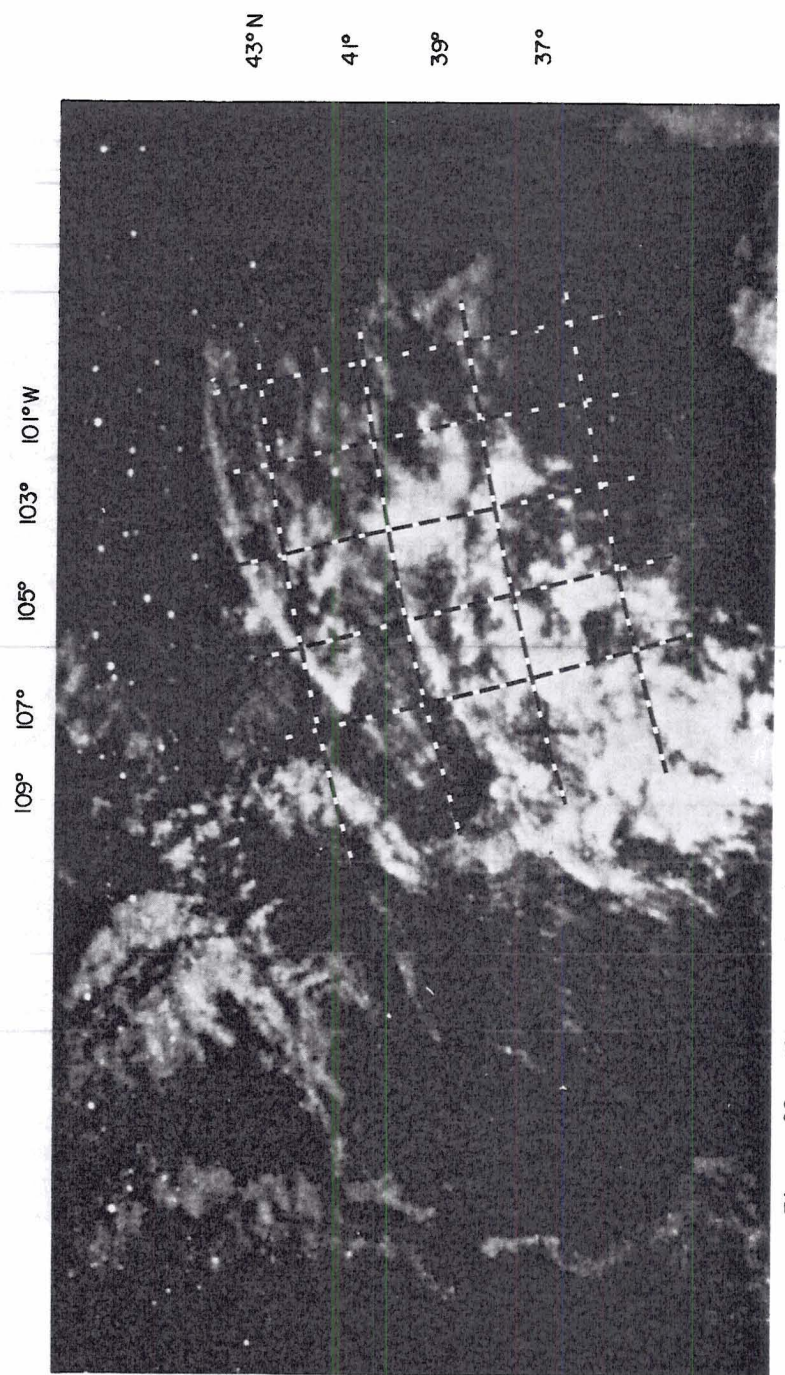


Figure 33. Photograph taken from ESSA VI satellite, 1805 GMT, 10 October 1968 (orbit 4199). (Note: Gulf of California, lower center; fog and cloud area off of southern California; and Great Salt Lake at 41N).

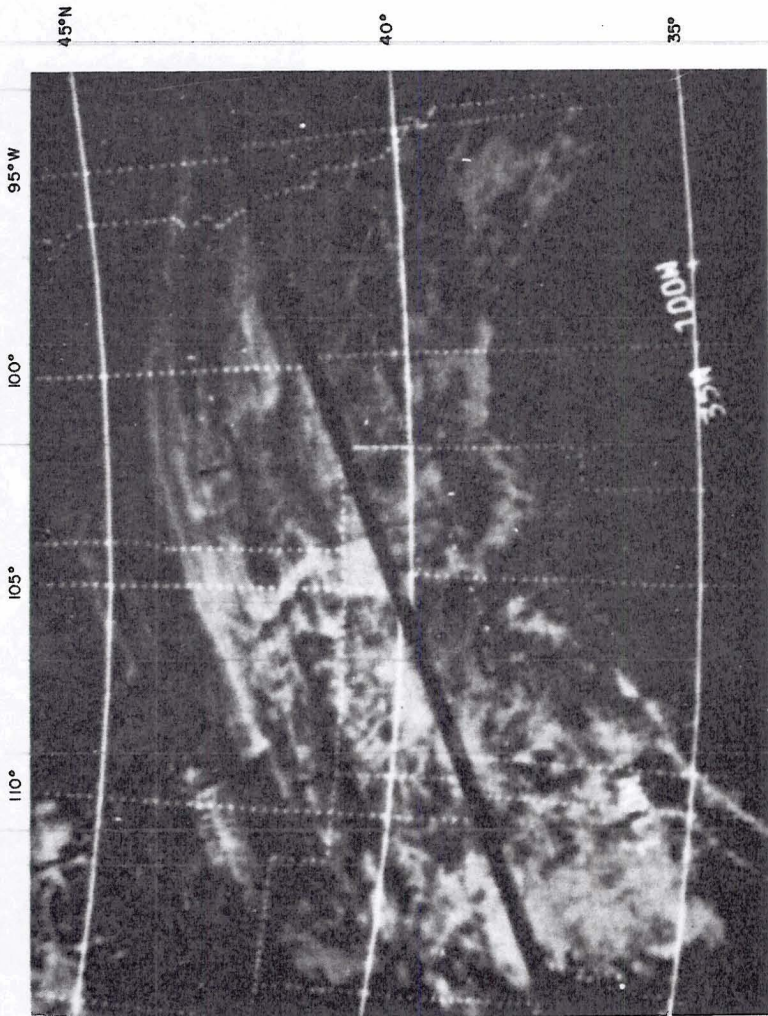


Figure 34. Photograph taken from ESSA VII satellite, 1925 GMT, 10 October 1968 (orbit 693). (In addition to Colorado lee wave area discussed in text, note the vertebratus at 43N, 110W)



time spent by The Explorer in a particular region during the investigation. The blocks are 50 mb in the vertical and 1 km in the horizontal. This figure was constructed to verify the wavelengths determined from the ozone and temperature data. The Explorer spent the majority of the flight time in areas of ascending motion, therefore the largest figure in the "sum of columns" row would represent the area of maximum wave lift. For example, in the row titled "sum of columns", the largest figure listed is 16.46. This indicates that The Explorer spent 16% of the three hour period in the region 22 to 23 km east of the Continental Divide. The number in the extreme upper left portion of the figure, 4.35, indicates that greater than 4% of the investigation time was spent in the region between 400 and 450 mb at 2 to 3 km east of the Divide.

By measuring the horizontal distance between the highest numbers in the "sum of columns" row, one indirectly determines the wavelength. Two wavelengths for the lee waves were determined in this manner. One wavelength measured 8.0 km, the other 11.8 km. The average is 9.9 km.

From The Explorer, the average cloud wavelength was estimated to be on the order of 10 km.

Foldvik [1962] has noted that theoretically the wavelength of the gravity wave must be  $> 2\pi/\ell_{\max}$ . Using this criterion, the minimum possible wavelength in the region of investigation was computed using the  $\ell_{\max}$  from Figure 28. The resulting wavelength was 4.6 km.

Corby [1957] gives a relationship between wavelength and mean tropospheric wind. This relation is:  $\lambda = \frac{U-10.5}{3.27}$ , where  $\lambda$  = wavelength in km, U = wind velocity in knots. From the Brainard Lake sounding the mean wind was computed to be  $20 \text{ ms}^{-1}$ . A check on this wind could be obtained by an analysis of the Niwot Ridge wind (Figure 36) during the flight period. This might be a better indication than the few minutes of wind data obtained from the ozonesonde. Niwot Ridge is at an elevation of 12,284 ft. It is 3.7 km NE of North Arapaho Peak (see Figure 8) and 5 km SW of Brainard Lake. During the flight, gusts were recorded as high as  $35 \text{ ms}^{-1}$ , however the mean wind was quite a bit less. The mean wind from 12 to 22 GMT indicated a slow decrease in intensity. However, during the investigation, from 17 to 20 GMT, an increased

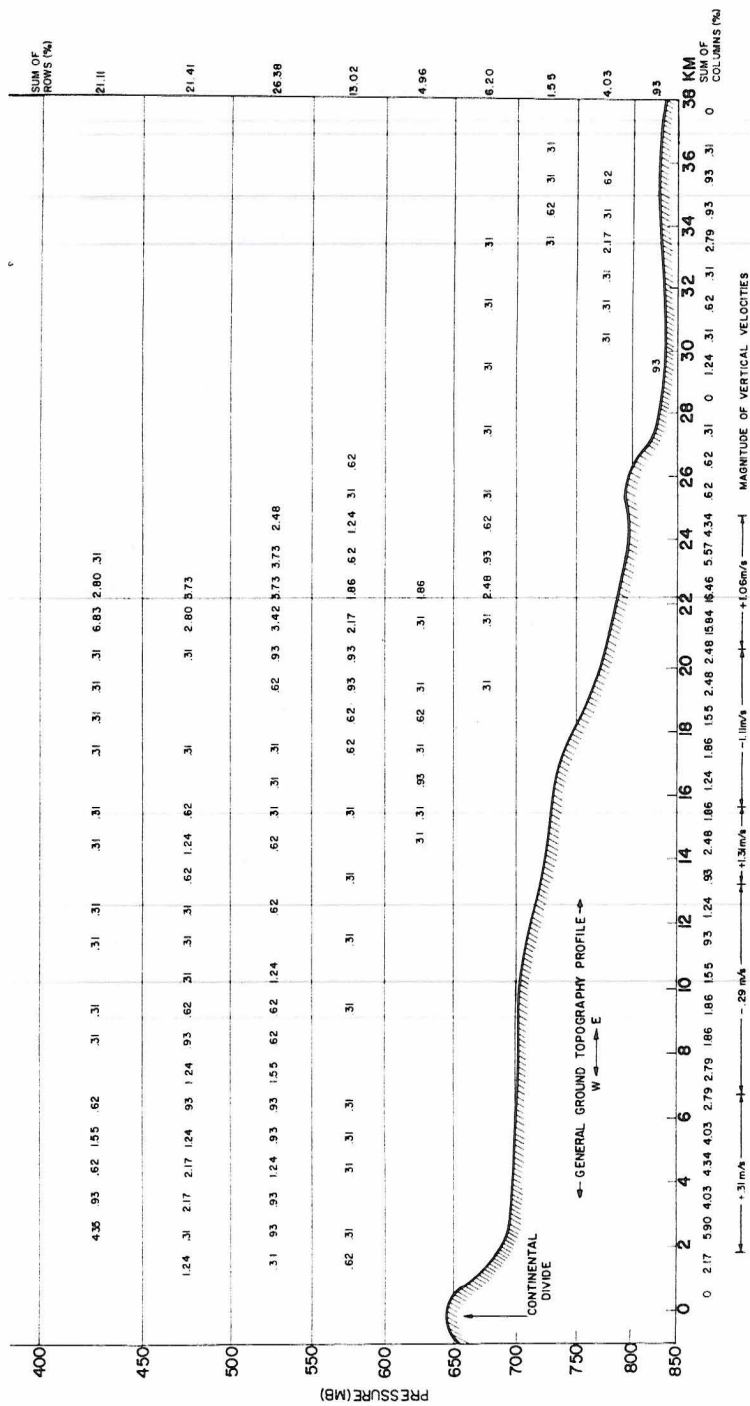


Figure 35. Cross-section east of the Continental Divide depicting frequency of location in a given increment of The Explorer during study, based on radar data, 10 October 1968 (see text for elaboration).

intensity was observed. The mean wind for the period was  $20 \text{ ms}^{-1}$ , compatible with that measured by the ozonesonde. The temperature from Niwot Ridge served as an additional check on the ozonesonde and aircraft temperature element.

Using a mean tropospheric wind speed of  $20 \text{ ms}^{-1}$ , the calculated wavelength, using Corby's criterion, was 8.7 km.

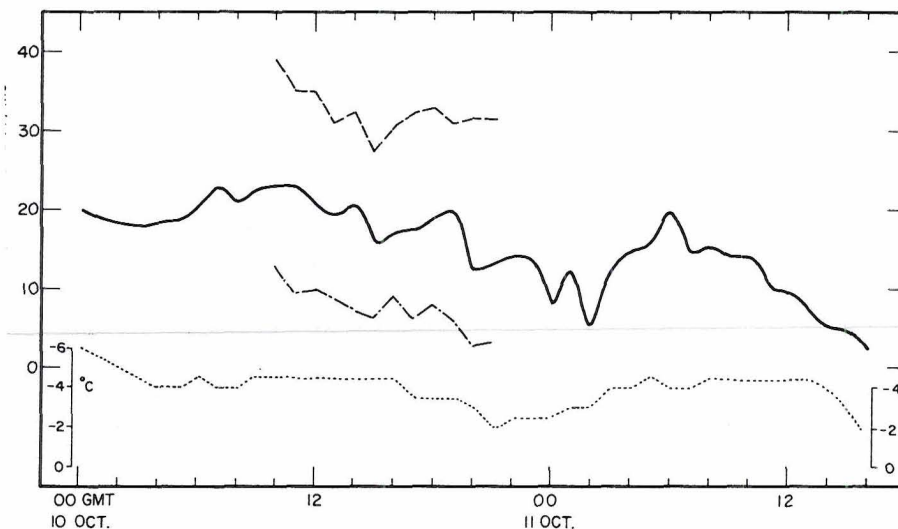


Figure 36. Niwot Ridge wind data 10 and 11 October, 1968. Heavy line represents mean hourly wind, long dashed line, the maximum wind, ash-dot line, the minimum wind, and the dotted line, the temperature.

Another technique to calculate the wavelength would be an indirect determination by means of vertical velocities obtained from the ozonesonde mean ascension rate. Departures from the mean ascension rate of the ozonesonde were determined and are indicated at the bottom of Figure 35. The magnitude of the vertical velocities is plotted horizontally, as the balloon trajectory carried the ozonesonde to the east. Regions of ascending and descending motions could thus be defined in yet another manner. Analysis of these areas indicated an average distance of 9.2 km from one area of maximum ascending motion to another.

Thus, the wavelength may be determined by seven different techniques. The average of all techniques, with exception of the satellite data, indicates a wavelength of 9.9 km. This compares to an average of 13.8 km for the satellite--a difference of only 3.9 km.

*Scorer* [1949, 1953, 1954], it should be noted, theorizes that the wavelength is determined entirely by physical atmospheric parameters and not by the dimensions of the disturbing obstacle.

It is noteworthy to mention that an undercast below a wave cloud can prevent discerning of the wave cloud in a satellite photograph. In certain portions of the wave region this was true on 10 October. The wave clouds and undercast cloud are seen in Figure 37.



Figure 37. Photograph of lee waves and other cloud forms (taken from *The Explorer* at 6.1 km (20,000 feet) MSL). (See text for elaboration)

Using Foltz's criteria for degree of clear air turbulence and computing  $w$  as suggested [Foltz, 1967], light turbulence should have been experienced on this date. During the six-hour period of flight in the lee waves, this seemed to be a realistic estimate.

*Amplitude.* One attempt was made to calculate the lee wave amplitude. Measured amplitudes from the ozone surfaces in Figure 29 indicated amplitudes from 0.5 to ~1.1 km. The 1.1 km amplitude was estimated because the wave crest had not been reached when the data terminated in the eastern portion of the flight area. A similar amplitude was indicated from the potential temperature surfaces.

Visually (determined from wave clouds viewed from The Explorer), the amplitude ranged from approximately 1/2 to 1 km.

*Vertical velocities.* Vertical velocities were determined by several methods. The horizontal wind from 400-600 mb (calculated from Brainard Lake sounding) was used in conjunction with the shape of the ozone partial pressure surfaces (Figure 29) to determine vertical velocity. This was calculated to be ~1-2  $\text{ms}^{-1}$ .

As mentioned earlier, vertical velocities could be obtained from the ozonesonde flight characteristics (Figure 3). Calculated in this manner were maximum positive (upward) vertical velocities of 1.3  $\text{ms}^{-1}$  and maximum negative (downward) vertical velocities of 1.1  $\text{ms}^{-1}$ .

In addition to the two above-mentioned techniques of determining vertical velocities in the lee wave, The Explorer was equipped with two rate of climb indicators. At 26-30,000 feet (7.9-9.1 km = 300-360 mb), upward velocities were 0.5-1.0  $\text{ms}^{-1}$ . At 18-26,000 feet (5.5-7.9 km or 360-500 mb), the average positive lift was ~1.5-2.5  $\text{ms}^{-1}$ . As low as 11,500 feet (3.5 km or 660 mb), lift moved The Explorer upward at 5.2  $\text{ms}^{-1}$ . The maximum vertical velocities measured by The Explorer occurred at three separate times and each lasted 1-3 minutes. The maximum vertical velocities were encountered at 15-18,000 feet (4.6-5.5 km or 500-570 mb) and were >10  $\text{ms}^{-1}$ .

It is logical that an instantaneous vertical velocity as measured by a sailplane will be considerably greater than vertical velocities averaged over a period of time and over several waves. Indeed, the average vertical velocity as determined by ozone and potential temperature surfaces and by ozonesonde ascent rates averaged 1.4  $\text{ms}^{-1}$ . A subjective analysis of the average lift of The Explorer places the lift for the 400-600 mb layer at 1-2  $\text{ms}^{-1}$ . The three techniques agree

remarkably well in indicating a vertical lift in the average lee wave during the study as  $-1.5 \text{ ms}^{-1}$ . A summary of wave amplitude, wavelength and vertical velocities is given in Table 2.

Table 2. Magnitude of wavelength, amplitude and vertical velocity as determined by methods below (see text for elaboration).

Method of Determination	Wavelength (km)	Amplitude (km)	Vertical Velocity ( $\text{ms}^{-1}$ )
1. Satellite			
ESSA VI	14.3		
ESSA VII	13.3		
2. Ozone Data	8.5 - 10.5	0.5-1.1	1 - 2
3. Potential Temperature Data	8.5 - 10.5	0.5 - 1.1	
4. Radar Data	8.0 - 11.8		
5. Theoretical Computation	8.7		
6. Ozonesonde Wind Data	9.2		1.1 - 1.3
7. Subjective Determination from Explorer	10	0.5 - 1.0	0.5 - >10 Average = 1 - 2

*Foldvik* [1962] has shown that the height at which the vertical velocity is a maximum is not a function of the height or shape of the mountain profile, however on the several flights in lee waves during the fall of 1968 in the same general area as this study, maximum

vertical lift was usually obtained at 4.5-6.0 km.

#### IV. Mountain-Induced Lee Waves and the 1.5 Million Dollar Destruction in Boulder, Colorado, 7 January 1969

The home exhibited in Figure 38 is but a small sample of the destruction brought about by extremely high winds that struck the Boulder community at 3 p.m. (22 GMT) on 7 January 1969. The scene in

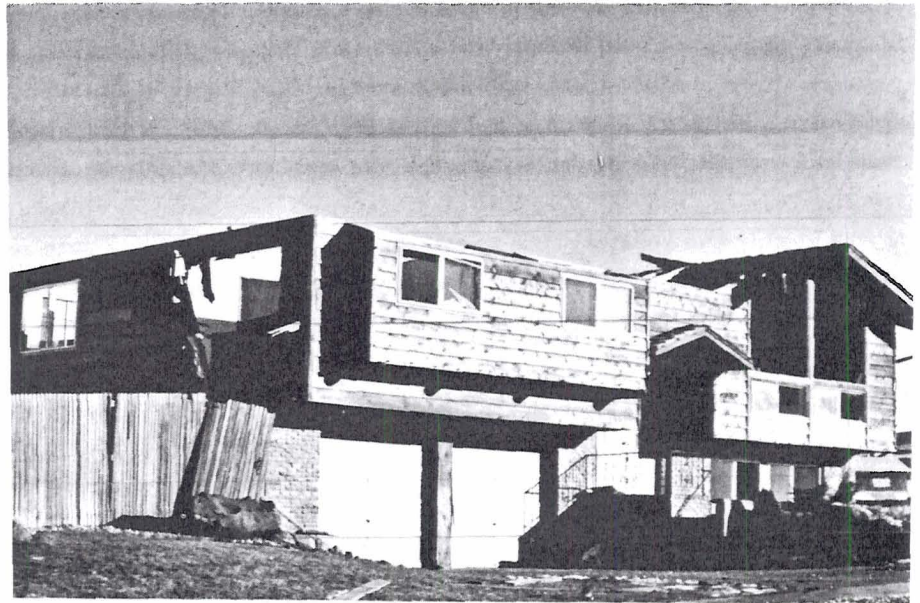


Figure 38. Photograph of destroyed home immediately after high wind conditions in Boulder (see text for elaboration).

Figure 38 was repeated dozens of times in more or less severity throughout west Boulder and particularly so in the Table Mesa area near the National Center for Atmospheric Research building. The tremendous force necessary to lift an entire roof from a house and deposit it many feet away certainly deserves investigation.

*Synoptic pattern.* Aloft at 500 mb, an intense cyclone moved into northwestern Canada on 27 December. By 29 December it was the dominant

feature in the upper air pattern over all of North America. The cyclone progressed eastward, and by 2 January it was just north of Nova Scotia. At this point, little movement was indicated over the next twelve-hour period. However by 3 January, it was obvious that it was indeed retrograding. By 7 January, retrogression had brought the trough westward to longitude 85 W. At this point, a deep trough was embedded in the flow extending from northern Canada into the Gulf of Mexico (see Figures 39, 40, 41). The high-level retrogression of this cyclone has been discussed at length because it is, in effect, the feature that set up a blocking situation, such that for nearly two weeks prior to 7 January the surface systems over the United States and particularly over Colorado were stagnant. A surface frontal system that had entered Colorado on 23 December had meandered slowly back and forth across the state. A trough at the surface remained in evidence to the lee of the Rockies. This was the synoptic situation for two weeks prior to 7 January and again the situation as seen in Figure 42 on 7 January.

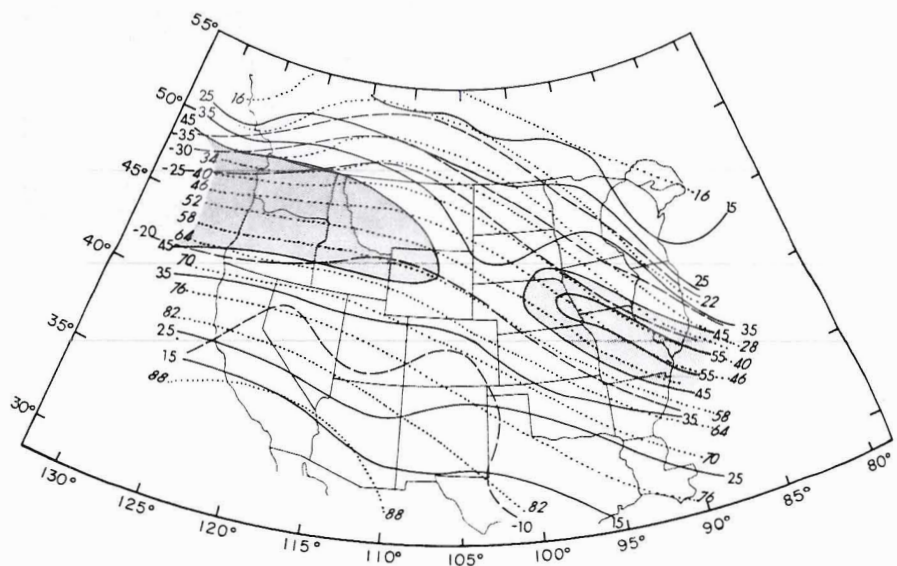


Figure 39. 500 mb isotach analysis, 12 GMT, 7 January 1969. Isotach ( $\text{ms}^{-1}$ ) - solid line, temperature ( $^{\circ}\text{C}$ ) - dashed line, contours (meters; first digit omitted for 500 and 300 mb, first two digits for 100 mb) - dotted line.) (Shaded areas  $> 45 \text{ ms}^{-1}$ )



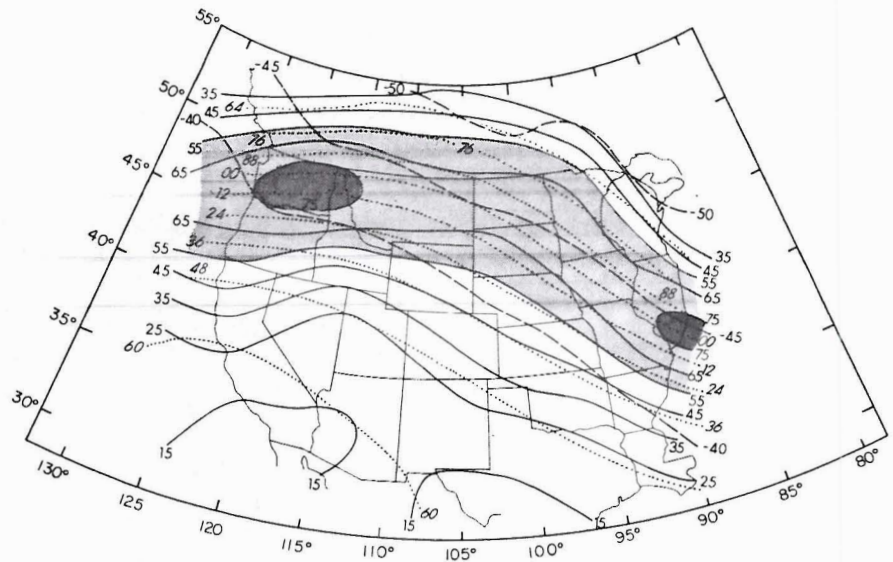


Figure 40. Same as Fig. 39 except 300 mb isotach analysis. (Light shaded area  $> 55 \text{ ms}^{-1}$ , heavy shaded area  $> 75 \text{ ms}^{-1}$ .)

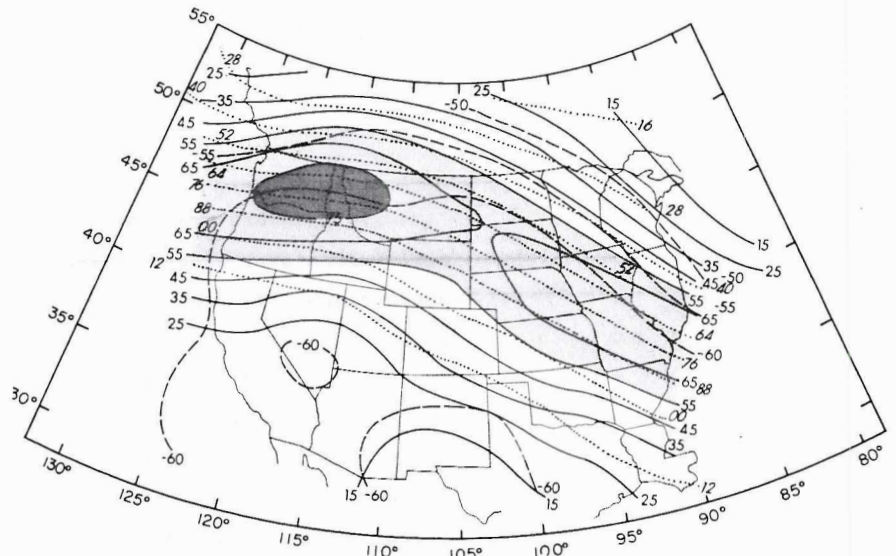


Figure 41. Same as Fig. 39, except 200 mb isotach analysis. (Light shaded area  $> 55 \text{ ms}^{-1}$ , heavy shaded area  $> 75 \text{ ms}^{-1}$ .)

On this day, a deepening trough is evident along the lee of the Rockies. The front associated with the trough was located just a few kilometers east of Denver in Figure 42. (This will easily be seen from evidence presented later.)

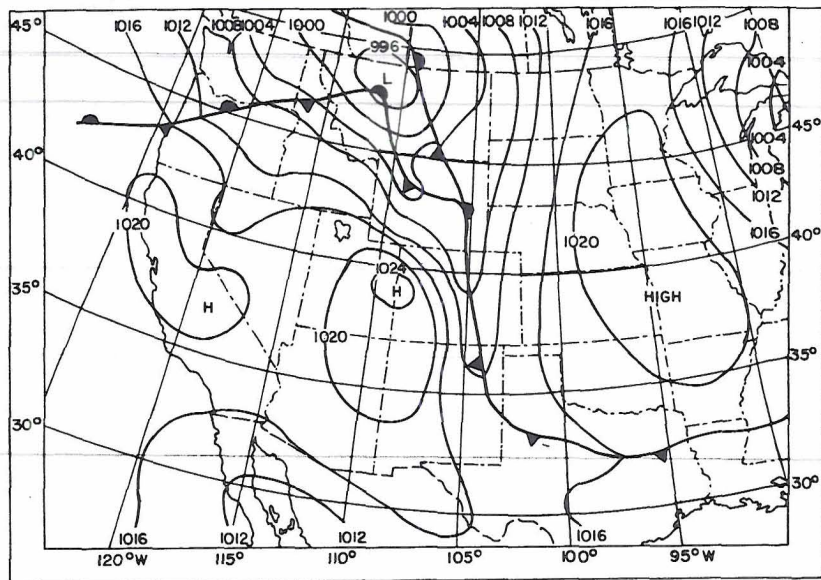


Figure 42. Surface synoptic chart for 12 GMT, 7 January 1969 (from SSA).

The pressure gradient at the surface was steepened further by an anticyclone over western Colorado. At 500 mb (Figure 39), the surface anticyclones (Figure 42) in California and western Colorado were reflected weakly in the temperature field. Most dominant at 500 mb is the bottom of the high-level jet entering the United States in the Pacific Northwest and penetrating as far as central Wyoming with  $50 \text{ ms}^{-1}$  winds. At 300 and 200 mb (Figures 40 and 41), the jet stream is noticeably reflected in the isotach analysis. Flow at 300 and 200 mb (9 and 12 km respectively) is northwesterly from the Great Basin to the Mississippi. A  $75 \text{ ms}^{-1}$  jet stream maximum is centered over Washington and northern Idaho at both levels.

On 8 January the upper level situation changed drastically. The trough, that had been moving slowly westward for about a week and that had been located at 80°N on 7 January at 12 GMT, moved rapidly eastward, and on 8 January at 12 GMT was at 65°W. The direct result was that systems at the surface were allowed to move rapidly southeastward. Aloft, the jet stream had moved some 600 km southeastward by 12 GMT on 8 January. The jet core was centered over northern Colorado and southern Wyoming as indicated at 300 and 200 mb (Figures 43 and 44). The leading edge of the jet over eastern Colorado and Nebraska exhibits a slight "fingery" structure (not shown in the analysis) at both the 300 and 200 mb level similar to splitting noted by *Reiter* [1963b]. The leading edge of the jet at 300 mb (7,000 meters over Colorado), with winds of 75 ms<sup>-1</sup>, is located over the Boulder area.

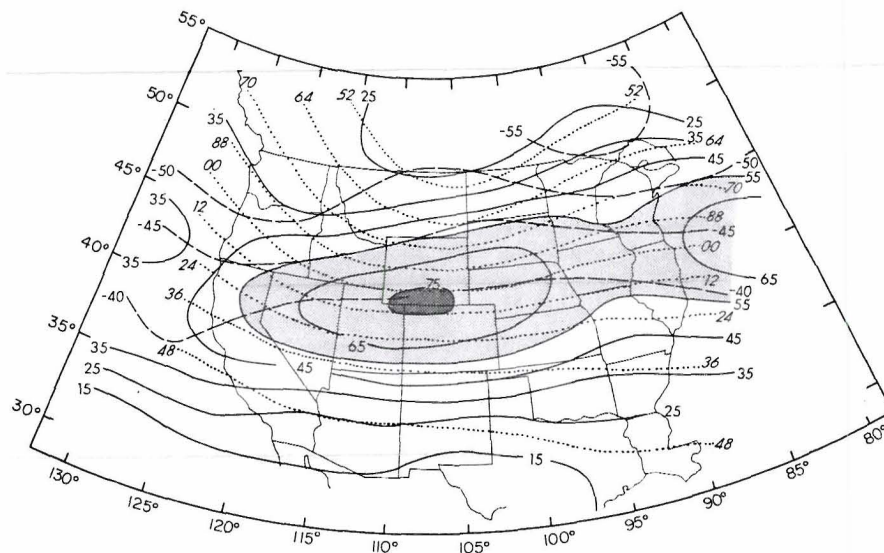


Figure 43. Same as Fig. 39, except 300 mb isotach analysis, 12 GMT, January 1969. (Light shaded area > 55 ms<sup>-1</sup>, heavy shaded area > 75 s<sup>-1</sup>.)

At 500 mb (Figure 45), a broad area of 45 ms<sup>-1</sup> winds is indicated by the isotach analysis. Quite noticeable is a very strong trough in

the isotherm field along the eastern slopes of the Rocky Mountains.

At the surface, the trough to the lee of the Rockies had intensified by 20 mb in 24 hours. By 12 GMT on 8 January, Figure 46 indicates the frontal system had just moved through the Boulder area.

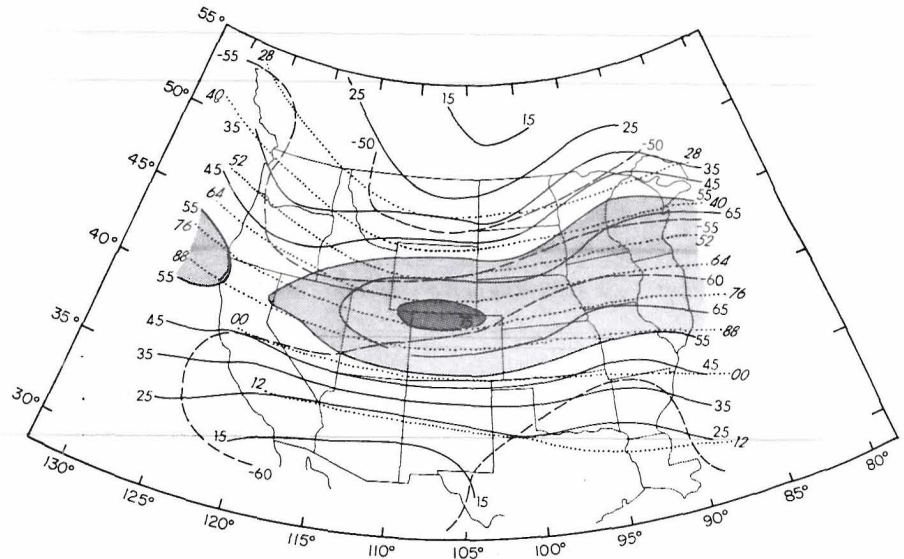


Figure 44. Same as Fig. 39, except 200 mb isotach analysis, 12 GMT, 8 January 1969. (Light shaded area  $> 55 \text{ ms}^{-1}$ , heavy shaded area  $> 75 \text{ ms}^{-1}$ .)

*Discussion of the Denver and Grand Junction soundings in relation to possible atmospheric conditions over Boulder on 7 and 8 January.*

Figures 47-52, for 7 and 8 January, depict resultant winds, potential temperatures, and the Scorer parameter with the reservations that  $\frac{1}{U} \frac{\partial^2 U}{\partial z^2}$  is to be neglected. The 7 January, 00 GMT (Figure 47),  $\ell^2$  indicates the best possible formation region for lee waves at Denver to be near the 250 mb level. At this time, it should be noted that neither were gusty winds recorded in Boulder nor were lee waves visible in the form of wave clouds. The simultaneous sounding for Grand Junction (Figure 48) indicated a quite similar  $\ell^2$  profile in the vertical. Twenty-four hours prior to the high winds in Boulder both stations

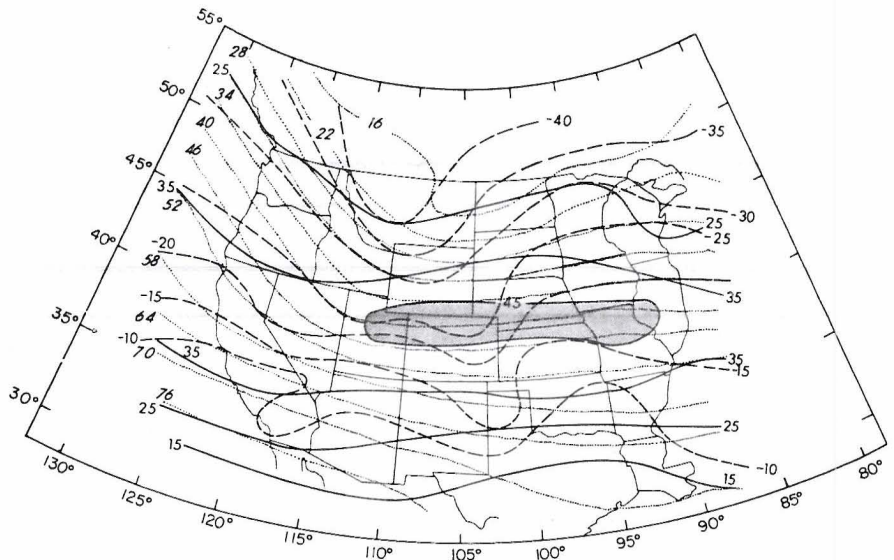


Figure 45. Same as Fig. 39, except 500 mb isotach analysis, 12 GMT, 8 January 1969.

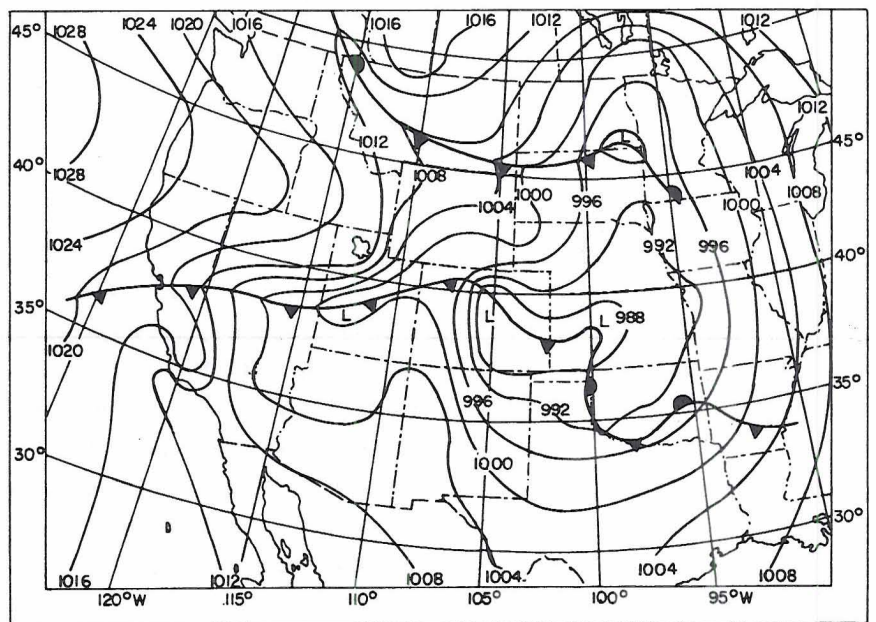


Figure 46. Surface synoptic chart for 12 GMT, 8 January 1969 (from ESSA).

report sufficient conditions favorable for lee wave formation, but no visible wave was observed. It should be noted that an inadequate resolution of the current upper air network makes the study of meso-scale phenomena difficult, but not impossible.

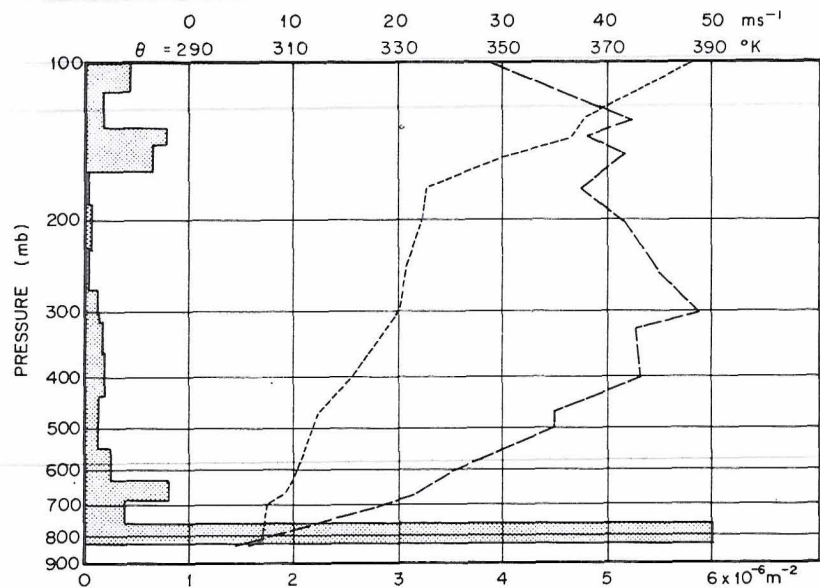


Figure 47. Same as Fig. 19, except for Denver, 00 GMT, 7 January 1969.

Twelve hours later (7 January, 12 GMT) the Denver  $\theta^2$  (Figure 49) indicated slightly more favorable lee wave formation conditions at 620 mb, 410 mb, 320 mb, and again around 250 mb. At this time no lee waving was noticed in cloud formations and surface winds at Boulder and Denver averaged less than  $3 \text{ ms}^{-1}$ . A very thin stable layer (200 meters thick) of air is seen immediately off the surface at Denver (Figure 49). From the height of this layer (810 mb) to the tropopause, the lapse rate is near adiabatic. A low level jet of  $31 \text{ ms}^{-1}$  is noted some 1700 meters off the surface.

Ten hours after the just discussed sounding, the wind increased sharply at Boulder (22 GMT, 7 January). At 00 GMT, 8 January, a

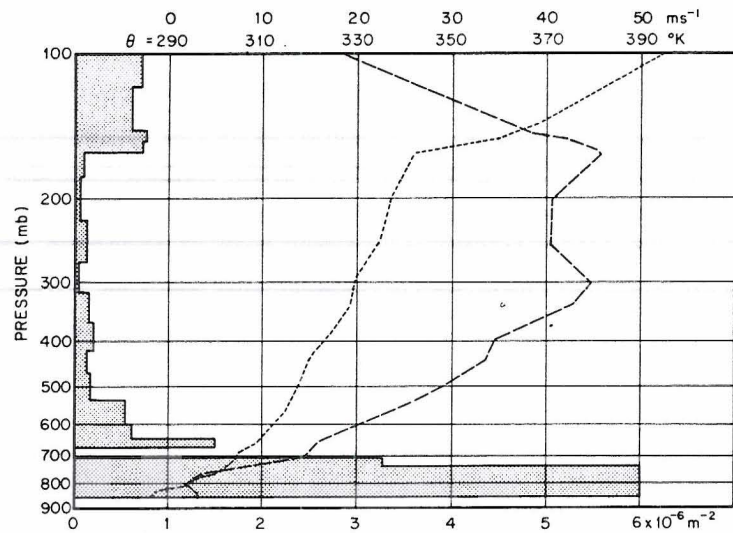


Figure 48. Same as Fig. 19, except for Grand Junction, 00 GMT, 7 January 1969.

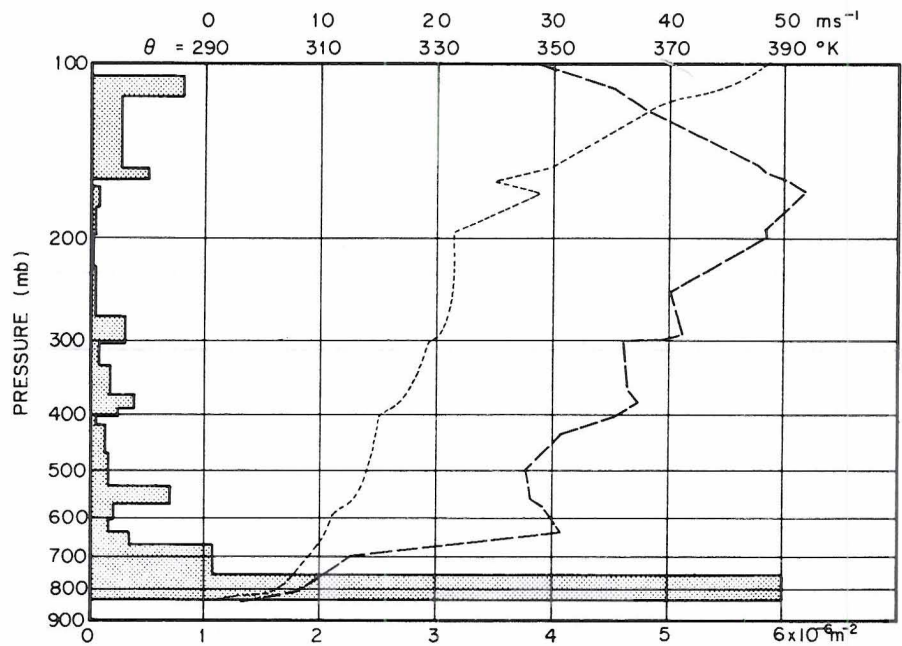


Figure 49. Same as Fig. 19, except for Denver, 12 GMT, 7 January 1969.

sounding was taken at Denver (Figure 50) and it revealed several interesting structures in the vertical: The Scorer parameter indicated the most favorable lee wave conditions in the past 72 hours. The Scorer parameter criterion was best satisfied at 560 mb. Although a thin stable layer exists for 100 meters off the surface (the winds were only  $5 \text{ ms}^{-1}$  at the surface), a deep layer of adiabatically mixed air exists up to the 630 mb level. The wind maximum of  $31 \text{ ms}^{-1}$  at 630 mb twelve hours previous, increased to  $42 \text{ ms}^{-1}$ , and moved up to the 500 mb level. The simultaneous Grand Junction sounding (Figure 51) indicates most favorable lee wave formations above 500 mb.

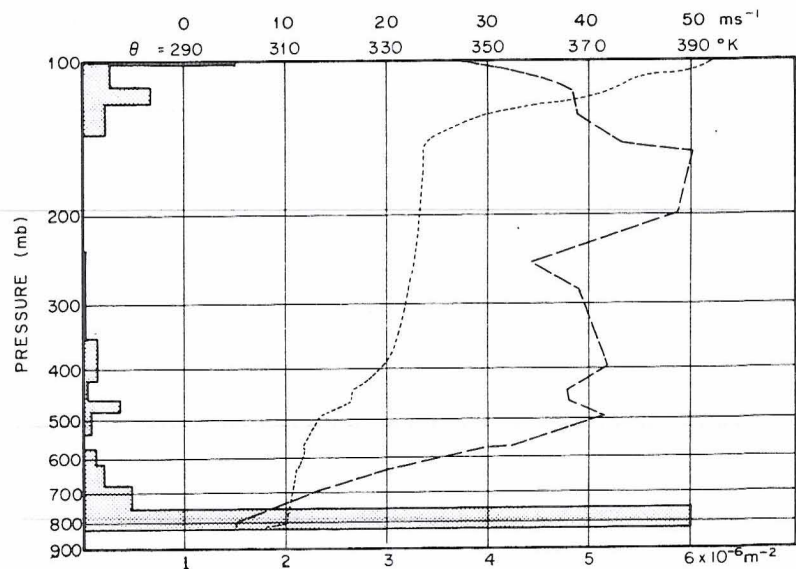


Figure 50. Same as Fig. 19, except for Denver, 00 GMT, 8 January 1969.

At 12 GMT on 8 January (six hours after the highest winds in Boulder had been recorded), the Denver temperature profile (Figure 52) indicated a deep adiabatic layer of dry air in the lower troposphere (surface to 540 mb). This is quite characteristic of a chinook current descending along the eastern slope of the Rocky Mountains [Reiter and



[Lahlman, 1965]. Winds at this time averaged  $16 \text{ ms}^{-1}$  at the surface and were gusty at Denver. Before limiting angles forced the termination of wind calculations, a velocity of  $64 \text{ ms}^{-1}$  was recorded at 380 mb.

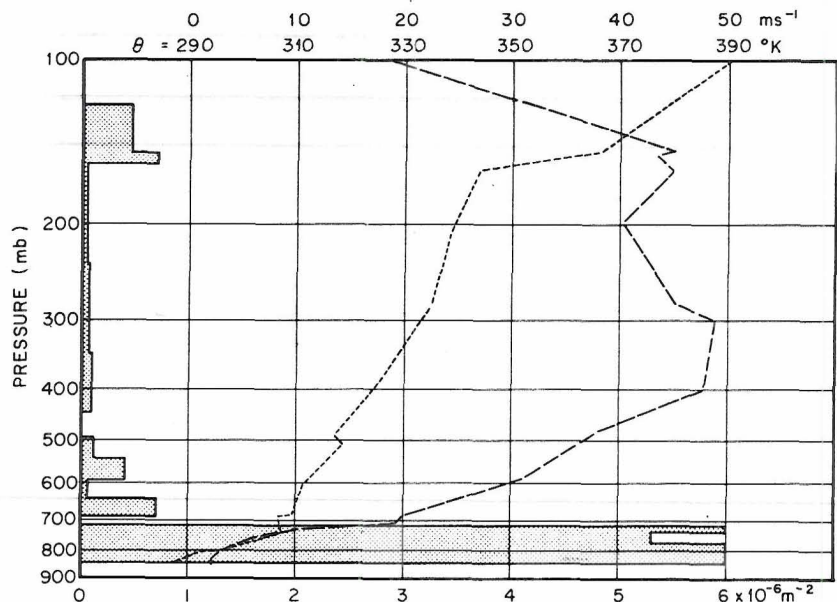


Figure 51. Same as Fig. 19, except for Grand Junction, 00 GMT, 8 January 1969.

Figures 53 and 54 present a vorticity and stability display simultaneously. Figure 53 indicates little vorticity gradient over Colorado on 7 January. Figure 54, however, reveals that by 8 January at 12 GMT the region was under the influence of a vorticity maximum. In addition, it should be noted that the Showalter stability index indicated an average for Colorado of +10 on 7 January at 12 GMT, by 12 GMT on 8 January the average was +4.5, and only +2 at Denver. This was the least stable area in the United States with exception of western Montana.

*Chinook conditions in the lee of the Front Range.* The eastern slopes of the Front Range, particularly near Boulder, were under the

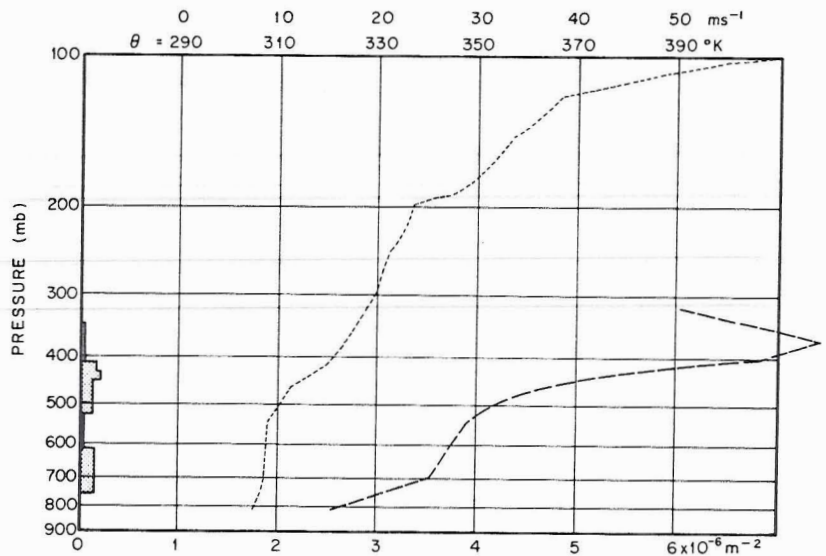


Figure 52. Same as Fig. 19, except for Denver, 12 GMT, 8 January .969.

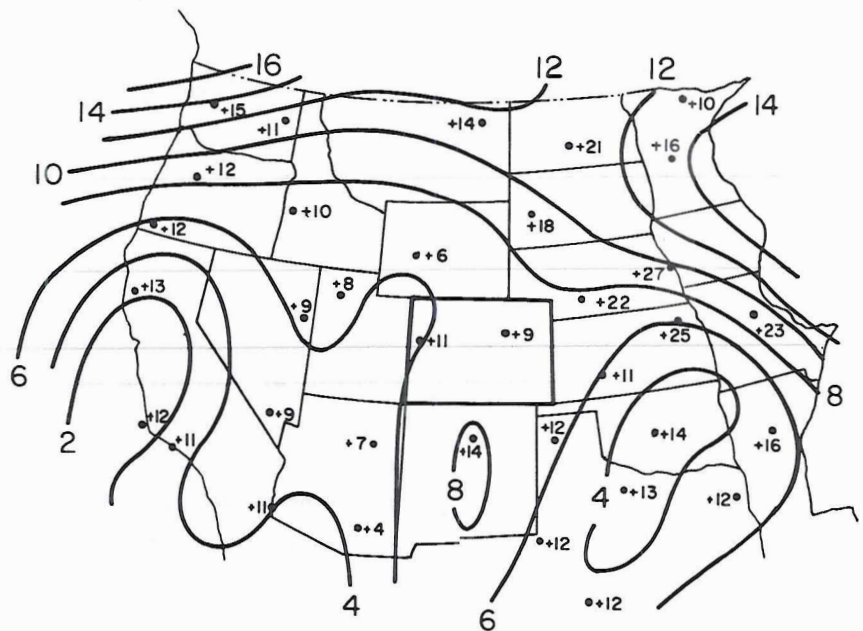


Figure 53. Vorticity ( $10^{-5} \text{ s}^{-1}$ ) and stability (from Showalter stability index) analysis for 12 GMT, 7 January 1969.

influence of a chinook from approximately 18 GMT on 7 January to 12 GMT the next day. This is seen in Figures 50 and 52. This chinook effect is easily seen along the eastern slope when Figure 55 is analyzed. This figure indicates a temperature gradient field such that each line represents a five degree temperature ( $^{\circ}\text{F}$ ) departure from the base temperature [ $21^{\circ}\text{C}$  ( $69^{\circ}\text{F}$ )] at stations along the eastern slope at 21 GMT (15 MDT).

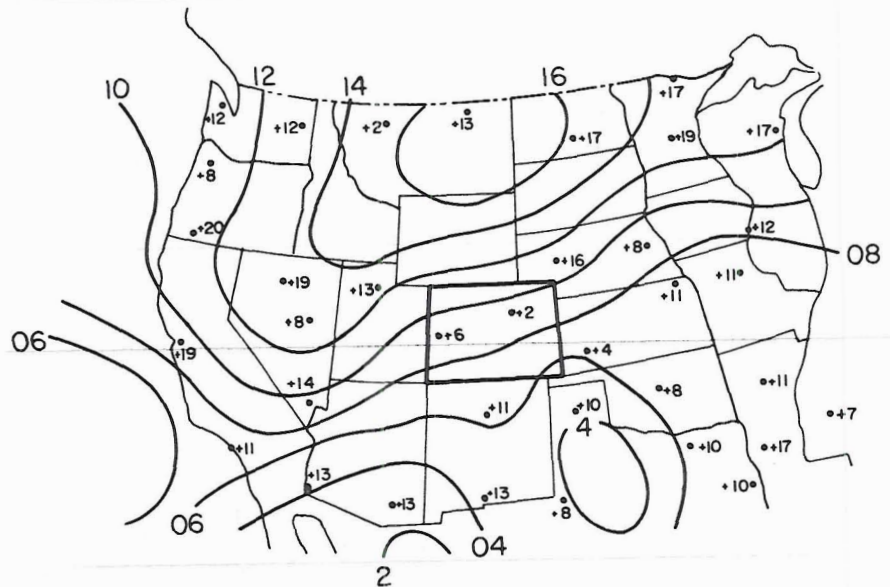


Figure 54. Same as Fig. 53, except for 12 GMT, 8 January 1969.

From an examination of Figure 55, realizing that all stations within the  $0^{\circ}$  isotherm were reporting gusty winds and large dew point reads, it appears likely that descending air motions on a large scale are occurring along the eastern slopes of the Rocky Mountains in a strong chinook current. Even a casual examination of Figure 55 indicates very large temperature differences east of the region immediately to the lee of the Rockies. A temperature difference of  $60^{\circ}\text{F}$  ( $33^{\circ}\text{C}$ ) is seen from the main chinook area to a region 800 km to the ENE. From

the chinook area to a point 105 km to the east a temperature difference of 30°F (17°C) is observed. This gradient points effectively to a remarkably sharp contrast between a pool of cold air advected from Canada at the surface over the eastern Plains and a warm region resulting from a strong subsiding current to the lee of the Rockies.

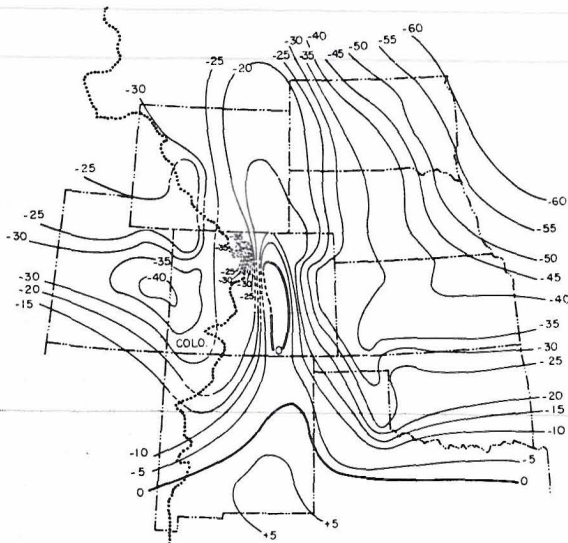


Figure 55. Temperature gradient field for Rocky Mountain and surrounding states for 21 GMT, 7 January 1969. (Base isotherm (°F) encircles 0 and north and Trinidad to the south.) (Figures represent departures from temperature within 0 line at 21 GMT.)

Figure 55 shows that the strongest dynamic heating by subsidence is from Boulder southward to Trinidad, Colorado, with a lesser effect over a larger area from Fort Collins into northeastern New Mexico. From Boulder westward to the Continental Divide a strong gradient seemed to exist. The data to provide this analysis were obtained from a permanent station atop the Continental Divide at 3,808 meters (12,493 feet) and from a station less than 5 km to its west at 3,449 meters (11,316 feet). The station atop the Continental Divide is at Colorado Mines Peak (46 km southwest of Boulder). The lower station is located at Berthoud Pass. Figure 56 gives a view of the area taken

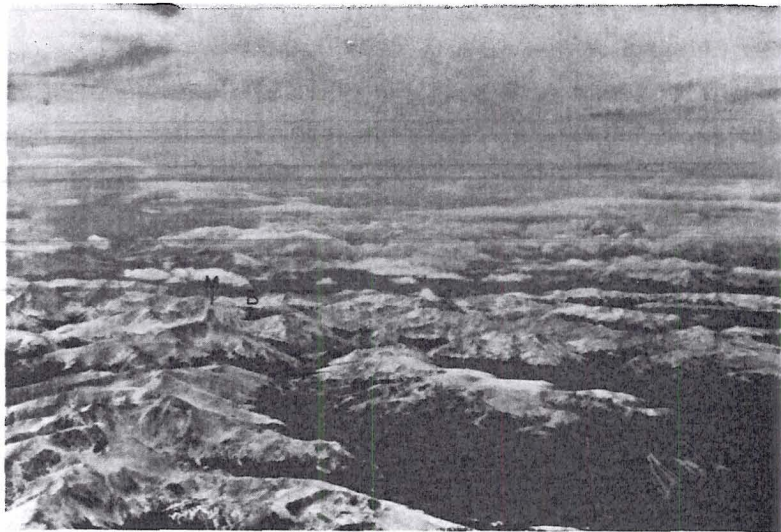


Figure 56. Photograph of Continental Divide and surrounding features from The Explorer at 7.6 km (25,000 feet) MSL. (Denoted in figure: Colorado Mines Peak (M); Berthoud Pass (B); also note ski area, lower right.)

from The Explorer at 7.6 km (25,000 feet) MSL. Mines Peak (denoted M in figure 56) is a very exposed area. It is here and at Niwot Ridge (discussed earlier) that the highest surface winds in Colorado are usually recorded. The Berthoud Pass station (denoted B in Figure 56) is more sheltered than Mines Peak. The data obtained from these two stations are presented in Figure 57. Only a wind recording system is available at the peak, however a temperature and barograph unit, in addition to a wind system, are located in the pass station.

According to Figure 57, the temperature at 21 GMT was  $+1.9^{\circ}\text{C}$  and at 22 GMT,  $+2.8^{\circ}\text{C}$ . These temperatures were the highest recorded in recent weeks at the pass and the  $2.8^{\circ}\text{C}$  temperature was only  $1.6^{\circ}\text{C}$  less than the highest ever recorded in January based on sixteen years of records at the 3,449 meter station. So, even with almost record maximum temperatures on the Continental Divide, a  $20^{\circ}\text{C}$  ( $35^{\circ}\text{F}$ ) temperature gradient existed between Boulder and mountain top level. This gradient was maintained mainly because many stations to the lee of the Front Range were recording the highest January temperature in years--in fact, many

stations set record maxima for the date.

Gusty winds were highest near the base of the Front Range and dew point spreads as mentioned earlier were quite large. Most dew point spreads within the 0°F gradient field to the immediate lee of the mountains (Figure 55) were greater than 25°C (45°F).

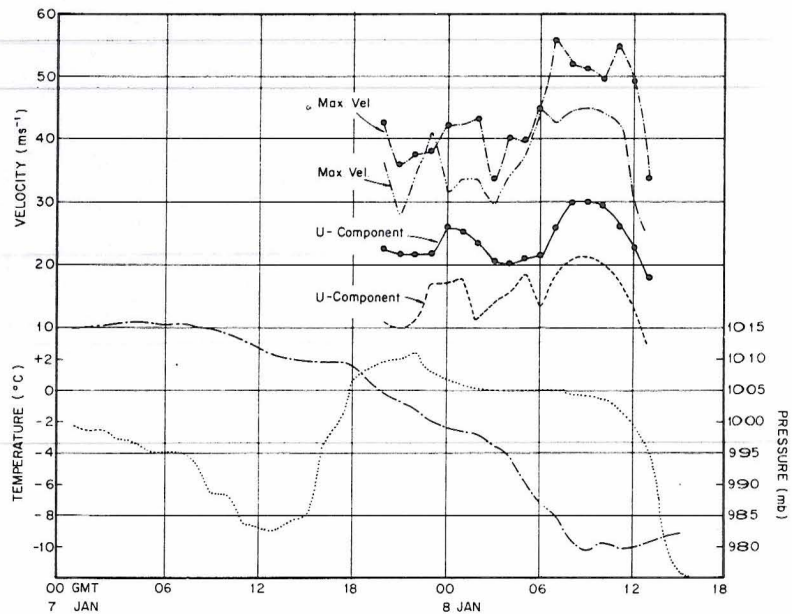


Figure 57. Plot of wind, temperature, and pressure at Mines Peak (3808 meters) and Berthoud Pass (3449 meters) 7 and 8 January 1969.

*Boulder and Mines Peak data.* Figure 58 presents various data at Boulder near the time of the high wind event. The Boulder data are obtained from a location atop the NCAR building situated on Table Mesa in SW Boulder at a height of approximately 1.89 km. Even a casual examination of Figure 58 results in several striking features: Wind gusts  $\geq 56 \text{ ms}^{-1}$  were recorded for a two-hour period. During the entire period of very gusty winds, the minimum velocity always returned to nearly  $0 \text{ ms}^{-1}$ . There was only a period of one hour during which sustained winds were able to maintain a speed greater than  $20 \text{ ms}^{-1}$ .

A more detailed examination of the Boulder data reveals the following.

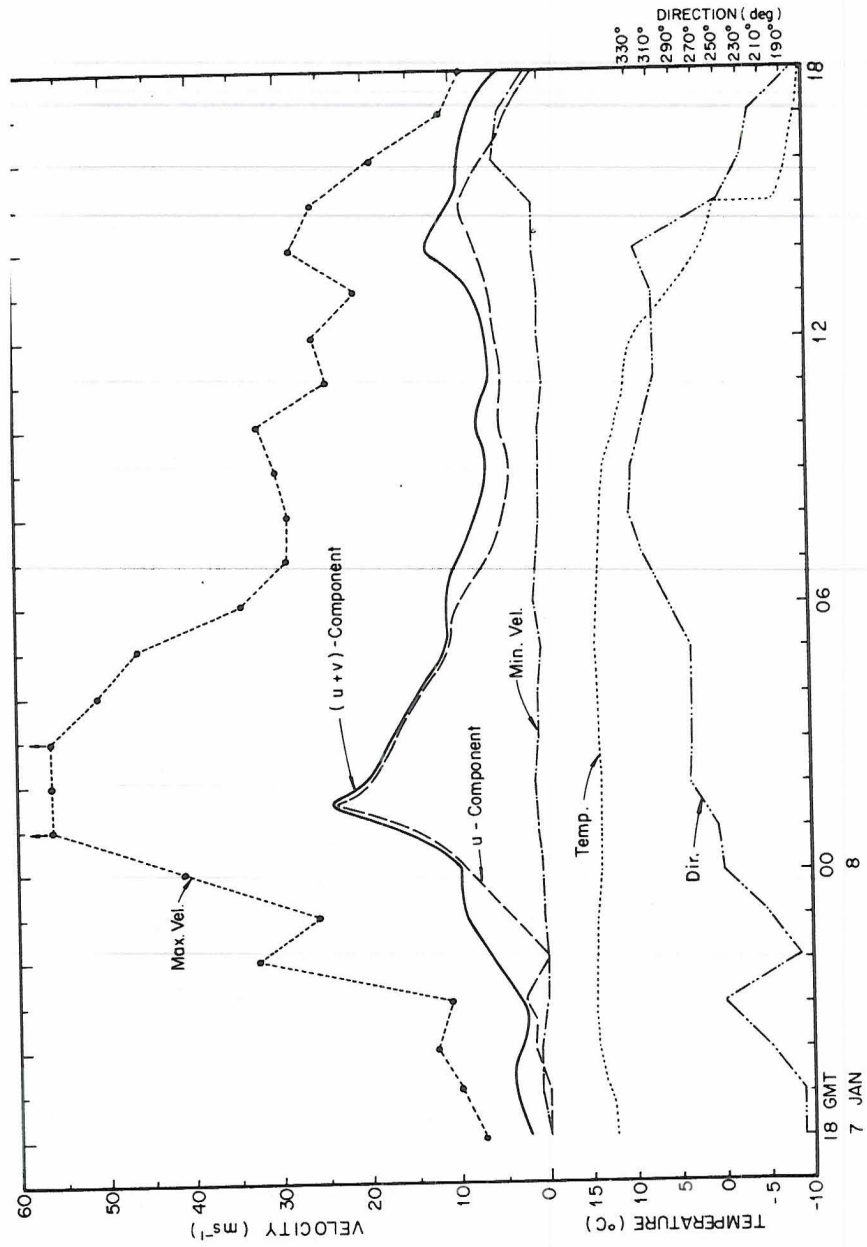


Figure 58. Plot of wind and temperature at Boulder, 7 and 8 January 1969.

At 21 GMT at the Table Mesa site, the average wind velocity (mean hourly resultant, u + v-components) was less than  $3 \text{ ms}^{-1}$  with gusts of only  $11 \text{ ms}^{-1}$ . In the next hour, while the average velocity was only  $7 \text{ ms}^{-1}$ , gusts of  $34 \text{ ms}^{-1}$  were occurring. By 00 GMT, 8 January, the peak gusts obtained a magnitude greater than the NCAR recording system could depict ( $>56 \text{ ms}^{-1}$  or 125 mph). By 0130 GMT the average resultant and u-component wind was  $25 \text{ ms}^{-1}$  with gusts  $>56 \text{ ms}^{-1}$ . From 01-04 GMT, there were 41 occasions on which the resultant wind gusts were  $45 \text{ ms}^{-1}$  and 19 occasions with  $>50 \text{ ms}^{-1}$ .

High winds were in evidence elsewhere during this period, particularly so at Mines Peak (Figure 57). The average wind (mean hourly u-component) at Mines Peak and Berthoud Pass reached maxima at 01 and 09 GMT. The u-component was determined because it gives a better estimate of velocities in the lee wave. This component during most of the period was quite close to the resultant wind (the flow at the top of the Continental Divide varied from  $260^\circ$ - $280^\circ$ ). The u-component 0.5 km below the peak at Berthoud Pass averaged  $\sim 8 \text{ ms}^{-1}$  less. The highest gusts at the Divide were  $>56 \text{ ms}^{-1}$  (Figure 57).

The first wind maximum at Mines Peak appeared to coincide within one hour of the Boulder maximum and, interestingly, the average velocity at both sites was the same. The high wind at the Divide seems, to a certain extent, to be reflected at the Boulder level as strong chinook, transferred from the 4 km level in lee waves.

Concentrating our attention on Boulder during the hours that wind gusts exceeded hurricane force ( $32.6 \text{ ms}^{-1}$ ), we find this period to last from 2330 GMT on 7 January to 0615, 8 January. Of the many gusts during the seven-hour period, almost all were immediately followed by a wind of little or no velocity. (The response time of a wind magnitude measuring system is not instantaneous; there is a lag on the order of a few seconds.) A typical example of the rapid variation in magnitude would indicate a practically calm condition followed approximately one minute later by a velocity of  $50$ - $55 \text{ ms}^{-1}$ . This condition might repeat itself five times in 10 minutes. The tremendous force exerted in more than an order of magnitude change over an interval of only one minute as one cause of the destruction in Boulder. The other was the



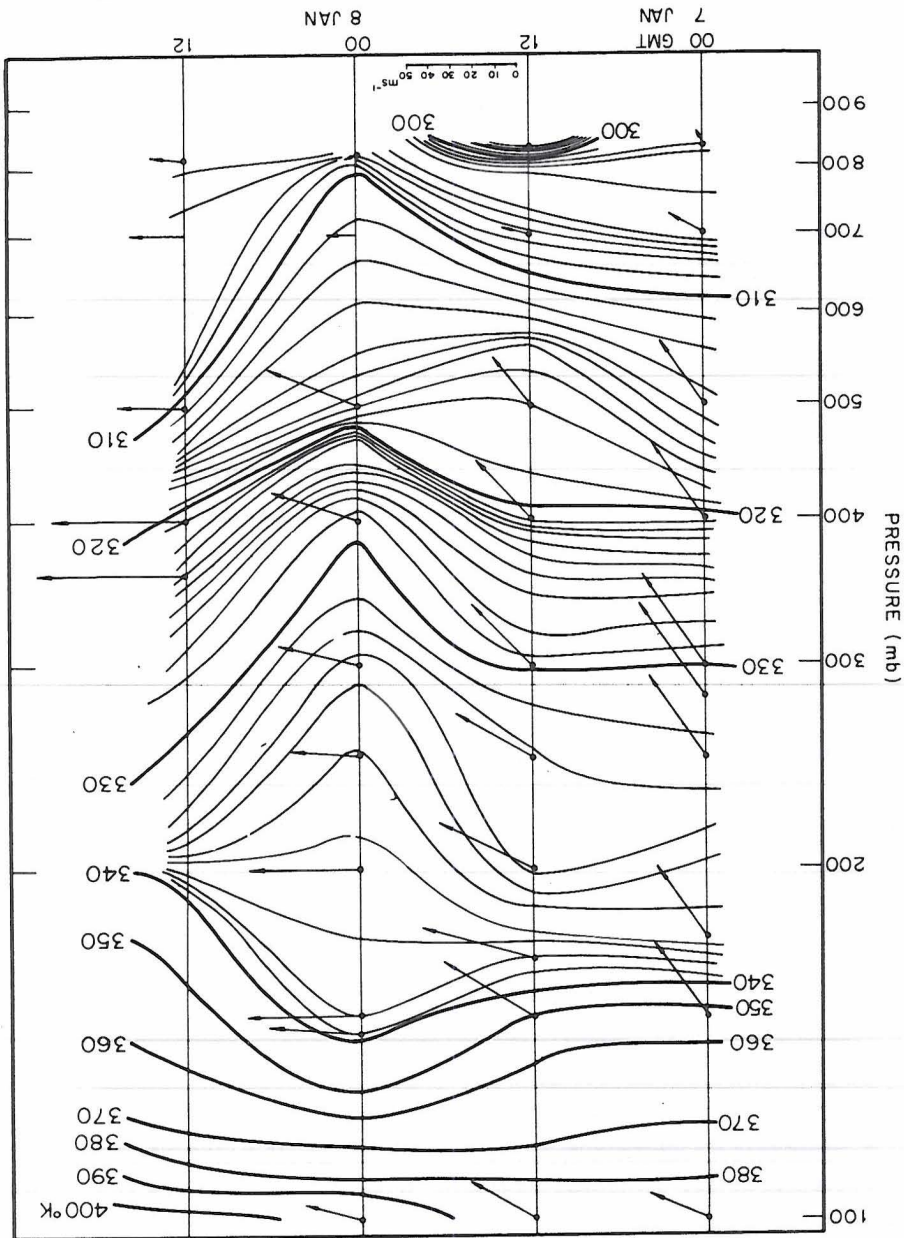
topography of the area. The most severe damage was in SW Boulder in the Table Mesa area. (Insurance companies place the loss at over 1.5 million dollars. Two persons were killed in the Boulder area as a direct result of the wind, and many were injured by the thousands of windows shattered.) A certain amount of channeling is effected by the canyons immediately to the west of Boulder. It appears that the strong downslope winds throughout the lee of the Front Range together with the strong channeling effect of canyons resulted in preferred regions of extremely gusty winds--probably in certain areas exceeding  $65 \text{ ms}^{-1}$ . Other areas in the immediate lee of the Front Range did report severe damage and estimates of winds of 150 mph ( $67 \text{ ms}^{-1}$ ), but in all cases the regions were only thinly populated and the total damage kept low compared to that of Boulder.

The gusty downslope winds decreased 50% by 06 GMT at Boulder. Strong winds from 8-16 GMT appeared to be more pre- and post-frontal than downslope. The frontal passage was rather dramatic at both the Mines Peak location and at Boulder. Trough passage appeared evident at Mines Peak (Figure 57) at 09 GMT. At this point, the lowest pressure was obtained (979 mb), mean wind and gusts decreased, and the temperature gradually began to fall. This appeared to be the approximate passage time at Boulder also. The dry, warm downslope condition appeared completely ended at 15 GMT when the temperature dropped  $7^\circ\text{C}$  in about 1/2 minutes.

#### The Transport of Stratospheric Air to the Surface by Orographical Effects

*Combined mechanisms.* Figure 59 is a mesoscale depiction of the vertical structure of potential temperature surfaces at Denver. A cross-section of the time section indicates subsiding motion at all levels below 175 mb beginning after 12 GMT on 7 January. The 333 K surface indicates isentropic motion from the 195 mb level at 12 GMT to the 305 mb level twelve hours later. By adoption of the proposed model for transport across the tropopause, as mentioned earlier, involving narrow filaments of stable, stratified air interjected into the troposphere from the stratosphere by wave action at the boundary, it is quite possible

Figure 59. Mesoscale vertical time section of the thermal structure from 00 GMT, 7 January to 12 GMT, 8 January 1969 (wind vectors also plotted).



that air with stratospheric characteristics could be found some 25-50 mb below the tropopause without evidence of the transport being reflected in a potential temperature field on a synoptic scale. It is also possible for quantities of stratospheric air to be associated with layers immediately below the tropopause, placed there by simple downward mixing in turbulent eddies in the high wind shear layers. Whether the stratospheric air arrived at the 195 mb level (some 35 mb below the tropopause) by laminar flow or eddies, or a combination of both, at referred times, once the air parcel is at this level, continued downward transport is available to the 300 mb surface. Once at this level, downward transport of momentum is available to the surface by gravity waves. [From a theoretical consideration, lee wave formation was likely at this time (see Figure 60 which depicts a time section of the variation with height of the Scorer parameter; note the downward slope of the gradient of the  $Q^2$  value with increasing time) and indeed, wave clouds are visible during this period.] Once the air was in the wave transport to the surface was inevitable in the powerful chinook current descending the lee slopes.

*Single mechanism.* Another possible method by which stratospheric air could be transported to the surface, and in a shorter period than the method just described, could be the following: As shown earlier in the October 1968 study, lee waving can drastically alter the height of the tropopause in the immediate lee of the mountains, and up to several hundred kilometers to the lee in some cases. In the near lee of the Front Range within the first 1-3 waves, the height of the tropopause would be changed most drastically. The October case indicates that this change may be as much as 1.5-2.0 km; the February 20 case (Figure 30) also indicates this to be 1-2 km. The obvious problem is that two stations 330 km apart (Grand Junction and Denver) are most useful for synoptic scale analysis and less so for measurement of mesoscale fluctuations. It is quite possible that both of these stations could fail to notice a disturbance in the Front Range, particularly if the disturbance was weak. (Radiosonde data smoothed by the coding process also permit small scale features to escape detailed analysis

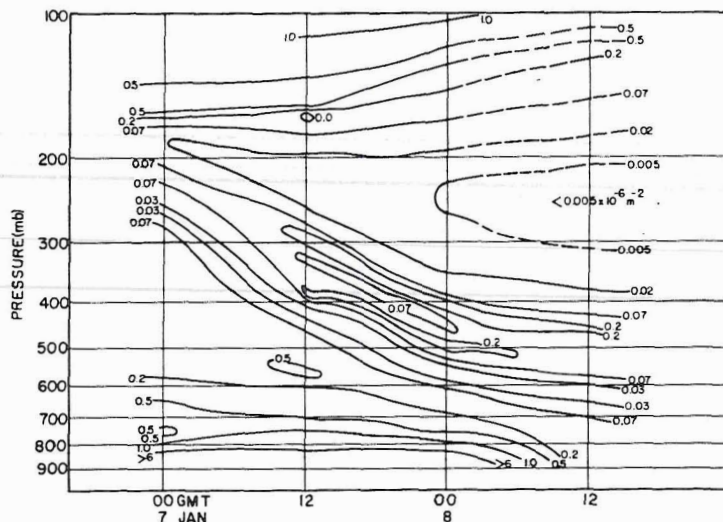


Figure 60. Mesoscale vertical time section of the Scorer parameter from 00 GMT, 7 January to 12 GMT, 8 January 1969.

[Danielsen, 1959]). Large changes in the tropopause height over short horizontal distances would go largely unnoticed upon inspection of the Denver sounding. (Although lee wave formation was indicated likely from theoretical treatment of the Denver sounding, no method was available to ascertain the degree of tropopause undulation.) Basically this mechanism suggests that lee waves, observed in occasional thin wave cloud form during the period of high surface winds, brought about large undulations in the tropopause. High winds at the top of the Front Range barrier would indicate longer wavelengths and in turn greater amplitude [Foldvik, 1962]. The high winds could also produce a breakdown of the basic wave flow into a more turbulent and chaotic flow pattern. Thus stratospheric air could be transported downward to the 300-350 mb level before 00 GMT, 8 January, while wind at mountain top level and in Boulder was less than  $25 \text{ ms}^{-1}$ . After this period, transport rapidly and directly to the surface in the lee of the Divide could be effected by eddy mixing in conjunction with the overall strong downslope chinook current along the lee slope.

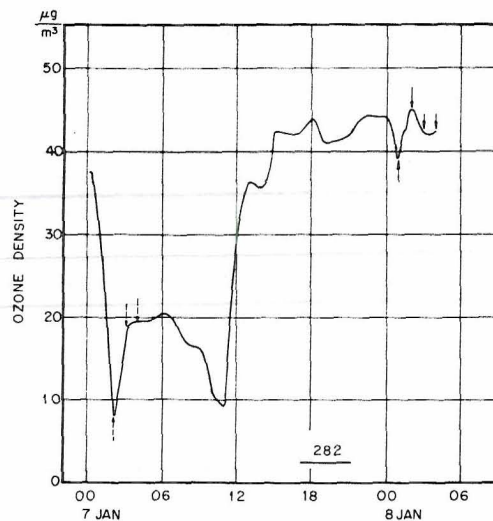


Figure 61. Plot of ozone density at the surface at Boulder, 00 GMT, January to 04 GMT, 8 January. (Dobson Spectrophotometer at 20 GMT = 82 m atm-cm.)

Figure 61 shows that air of recent stratospheric origin arrived at the surface along the eastern slope of the Continental Divide. Figure 61 depicts the fluctuation of ozone density with time. Since the surface serves effectively as a sink to ozone, as described earlier, the lowest ozone densities near the surface would be expected to occur during the night hours when convective activity is least and surface winds are weakest. This appears to be the circumstance early on 7 January. Evident is the maintenance of low ozone densities at night from 00-11 GMT). At 11 GMT (05 MST) on 7 January, the ozone density increases rapidly and rises some 350% by 18 GMT. During this same period the wind began to gust at  $7-13 \text{ ms}^{-1}$ . The ozone sensor shelter was blown over at 04 GMT on 8 January and measurements were terminated at that point. But before this occurred, it should be noted that ozone values were very high for that time of the day. In fact, densities were two to three times greater than 24 hours earlier. Some of this increase could be due to mixing at the surface. But it is felt that the

majority of the increase is indicative of stratospheric ozone reaching the surface as a result of one of the mechanisms discussed earlier.

#### VI. Summary

*Structure of the lee wave (case study 10 October 1968).* During the fall of 1968 a highly instrumented sailplane with ozone and temperature sensors was used to determine lee wave structure east of the Continental Divide in Colorado. One such case study is presented here.

A new type of ozone sensor, lightweight and potentially capable of measuring ozone on an absolute scale, was used on the aircraft. Unique sensor flow rate fluctuations under various aircraft maneuvers were conducted. It was found that variations were negligible.

This study for the first time obtained a rendezvous of an ozone sensor in an aircraft with an ozonesonde released from the surface. In addition, this was simultaneous with a photograph taken by ESSA VI. Additional satellite data, one to two hours prior to and after ozonesonde release, and during the aircraft sampling period, are analyzed.

A lee wave pattern is constructed based on a wave flow suggested by ozone partial pressure (and potential temperature) surfaces. This pattern verified the computed Scorer parameter which indicated atmospheric conditions suitable for the formation of lee waves. Ozone values were more useful in obtaining the lee wave structure than potential temperatures under adiabatic lapse rate conditions.

Five zones of different atmospheric processes in the ozonosphere are delineated from the vertical ozone structure.

From satellites, aircraft, sensors, ground-based radar, and an ozonesonde, seven independent techniques were used to determine lee wave amplitude, wavelength and vertical motion. The average wavelength from all methods, excluding the satellite information, was 9.9 km; ESSA VI and VII indicated an average wavelength of 13.8 km. Amplitudes varied from 0.5-1.0 km. From all available methods the average vertical velocity was computed to be  $1.5 \text{ ms}^{-1}$ . Extreme magnitudes greater than  $10 \text{ ms}^{-1}$  were recorded.

*Surface destruction and orographically-induced transport processes (case study of 7 January 1969).* Scorer parameters computed for 7 and 8

January indicated that the probability of lee waves during the period was quite good, particularly near the end of the observation period. It was quite evident by temperature and dew point analysis in the lee of the Colorado Rockies that chinook conditions were occurring. Analysis of wind data from the top of the Continental Divide, 46 km west of Boulder, and from Boulder, indicated near simultaneous occurrences of peak winds.

The high winds in Boulder produced quite extensive destruction because of two factors: (1) the wind was highly variable in magnitude--an almost calm wind would be followed a few seconds later by a gust, at times greater than  $56 \text{ ms}^{-1}$ ; (2) a channeling effect by the canyons to the west of Boulder substantially increased the wind in certain areas.

An explanation of the high surface wind was suggested in two proposed mechanisms. Both mechanisms provide for a rapid transport of stratospheric air to the surface. The first mechanism involved several processes in transport to the surface. Air was suggested to have been transported from the lower stratosphere (west of the Continental Divide) to the upper troposphere either by (1) a process allowing intrusion of thin stable laminae, or (2) erosion at the tropopause (both processes (1) and (2) could have occurred, each at preferred times). Once at a level a short distance below the tropopause large scale subsidence, observed by analysis on 7 January, would provide for transport to lower levels. At this point transport could be provided to the surface by large scale descending air motions in the lee of the Continental Divide brought about by lee wave-intensified chinook flow. The second mechanism suggested was that lee wave amplitudes were large enough to transport stratospheric air several kilometers downward, and from this point to the surface by large scale turbulent effects in the chinook flow.

It is certain that air of recent stratospheric origin arrived at the surface along the lee of the Front Range. This is reflected in surface ozone concentrations at Boulder during the observation period.

#### I. Suggestions for Future Research

Theoretical models have been derived that indicate possible flow under various atmospheric thermal and wind situations. However, detailed

study into the lee wave phenomena using highly equipped aircraft with atmospheric tracing capabilities is rare. More basic research into the formation and structure of the lee wave is needed using techniques described in this paper. Additional basic research into lee wave phenomena could show the coupling between such waves and high surface winds and chinook conditions in the lower troposphere and clear air turbulence in the upper troposphere and in stratospheric regions. In these higher regions turbulence could have severe consequences upon future SST flights.



### Acknowledgments

The author wishes to express his gratitude to Prof. E. Reiter (CSU) for perceptive discussion and valuable suggestions; to Drs. D. Lilly (NCAR) and J. Kuettner (ESSA) for introduction to and stimulating discussion of the gravity wave; and to Dr. W. Toutenhoofd (NCAR), the experienced pilot of The Explorer, for his time and advice. Sincere thanks must be expressed to Mr. W. Komhyr and his staff of ESSA, APRCL for their invaluable suggestions, for providing ozonesondes, for a special designed aircraft sensor and for the use of his facilities. Appreciation is expressed to Dr. D. Lenschow (NCAR) for aid in construction of a special temperature sensor; to Messrs. D. Sartor (NCAR), A. Judson (USFS), and M. Fosberg (USFS) for aid in obtaining Continental Divide meteorological data. Appreciation is also expressed to NCAR for computer time and radar and radiosonde facilities and personnel. Thanks must be expressed by the author and the scientific community, interested in the study of gravity waves and their effects, to Mr. K. Scribner for his conception of The Explorer and to Mr. G. Wallace for his financial support in construction of the aircraft. The FAA personnel at the Denver Center were extremely helpful for air traffic routing of The Explorer above 24,000 feet. Discussion of satellite and lee wave data by Messrs. G. Wooldridge and P. Lester has been useful. Thanks to Mrs. . Stollar and Mrs. H. Akari for the typing of the manuscript and for rafting work, and to Mr. J. Jennings and P. Lassauer for data compilation.

This research was sponsored by the National Environmental Satellite Center, ESSA, under Grant E-10-68G, and by the U.S. Atomic Energy Commission from Contract AT(11-1)-1340.

## References

- anonymous, 1968: Into the Maelstrom, *Pan Am Clipper*, Number 16, 28, pp. 9-11.
- reiland, J.G., 1968: Some large-scale features of the vertical distribution of atmospheric ozone associated with the thermal structure of the atmosphere. *J. Geophys. Res.*, Vol. 73, pp. 5021-5028.
- onover, J.H., 1964: The identification and significance of orographically induced clouds observed by TIROS satellites. *J. Appl. Meteor.*, Vol. 3, pp. 226-234.
- orby, G.A., 1954: The airflow over mountains. *Q.J. Roy. Meteor. Soc.*, Vol. 80, pp. 491-521.
- \_\_\_\_\_, 1957: A preliminary study of atmospheric waves using radiosonde data. *Q.J. Roy. Meteor. Soc.*, Vol. 83, pp. 49-60.
- anielsen, E.F., 1959: The laminar structure of the atmosphere and its relation to the concept of a tropopause. *Arch. Meteor. Geophys. Bioklimatol.*, All, pp. 293-332.
- illemuth, F.J., D.R. Skidmore and C.C. Schubert, 1960: The reaction of ozone with methane. *J. Phys. Chem.*, 64, pp. 1496-1499.
- oldvik, A., 1962: Two-dimensional mountain waves - a method for the rapid computation of lee wavelengths and vertical velocities. *Q.J. Roy. Meteor. Soc.*, Vol. 88, pp. 271-285.
- Foltz, H.P., 1967: Prediction of clear air turbulence. Atmospheric Science Paper No. 106, Atmospheric Science Dept., Colorado State University, Fort Collins, 145 pp.
- Hering, W.F., 1966: Ozone and atmospheric transport processes. *Tellus*, Vol. 18, pp. 329-336.
- Junge, C.E. and J.E. Manson, 1961: Stratospheric aerosol studies. *J. Geophys. Res.*, Vol. 66, pp. 2163-2182.
- Komhyr, W.D., 1964: A carbon-iodine ozone sensor for atmospheric soundings. Int. Ozone Symposium, Albuquerque, N.M., August.
- \_\_\_\_\_, 1967: Personal correspondence.
- \_\_\_\_\_, R.D. Grass and R.A. Proulx, 1968: Ozone intercomparison tests. *ESSA Technical Report*, ERL 85-ADCL 4, 74 pp.
- Kroening, J.L. and E.P. Ney, 1962: Atmospheric ozone. *J. Geophys. Res.*, Vol. 67, pp. 1867-1875.
- Kruger, P. and A. Miller, 1966: Transport of radioactivity in rain and air across the trade wind inversion at Hawaii, *J. Geophys. Res.*, Vol. 71, pp. 4243-4255.

- Lea, D.A., 1968: Vertical ozone distribution in the lower troposphere near an urban pollution complex. *J. Appl. Meteor.*, Vol. 7, pp. 252-267.
- Lilly, D.K., 1968: Lee waves in the Colorado Rockies. Presented at Symposium on clear air turbulence and its detection, 14-16 August, Seattle, Washington, 9 pp.
- Lovill, J.E., 1968: The vertical distribution of ozone and atmospheric transport processes over the San Francisco Bay area. Presented at the 48th annual meeting of the American Met. Soc., San Francisco, California, 29 Jan.-1 Feb.
- \_\_\_\_\_ and A. Miller, 1968: The vertical distribution of ozone over the San Francisco Bay area. *J. Geophys. Res.*, Vol. 73, pp. 5073-5079.
- Lyra, G., 1943: Theorie der stationären Leewellenströmung in freier Atmosphäre, *Z. angew. Math. Mech.*, Berlin, 23, p. 1.
- Machta, L., 1966: Some aspects of simulating large scale atmospheric mixing. *Tellus*, Vol. 18, pp. 355-361.
- Newell, R.E., 1963: The general circulation of the atmosphere and its effects on the movement of trace substances. *J. Geophys. Res.*, Vol. 68, pp. 3949-3962.
- \_\_\_\_\_, H.W. Brandli and D.A. Widen, 1966: Concentration of O<sub>3</sub> in the surface air over Greater Boston in 1965. *J. Appl. Met.*, Vol. 5, pp. 740-741.
- Neetzold, H.K., 1953: Die vertikale Verteilung des atmosphärischen Ozons nach dem photochemischen Gleichgewicht. *Geofis. Pura e Appl.*, Vol. 24, pp. 1-14.
- Northcock, A.B., 1966: A thin stable layer of anomalous ozone and dust content. *J. Atm. Sci.*, Vol. 23, pp. 538-542.
- Penney, P., 1947: Theory of perturbations in stratified currents with applications to air flow over mountain barriers. University of Chicago, Dept. of Meteorology, Misc. Report No. 23, 81 pp.
- Reger, V.H., 1941: Ozonshicht und atmosphärische Turbulenz. *Ber. d. deut. Wetterdienstes US-Zone no. 11*, pp. 45-57.
- \_\_\_\_\_, 1957: Vertical flux of atmospheric ozone. *J. Geophys. Res.*, Vol. 62, pp. 221-228.
- Reiter, E.R., 1963a: Nature and observation of high-level turbulence especially in clear air. Atmospheric Science Tech. Report No. 41, Atmospheric Science Dept., Colorado State University, Fort Collins, 26 pp.

- Reiter, E.R., 1963b: *Jet Stream Meteorology*. Chicago and London, The University of Chicago Press, 515 pp.
- \_\_\_\_\_ and H.P. Foltz, 1967: The prediction of clear air turbulence over mountainous terrain. *J. Appl. Met.*, Vol. 6, pp. 549-556.
- \_\_\_\_\_ and R.W. Hayman, 1962: On the nature of clear air turbulence (CAT). Atmospheric Science Tech. Report No. 28, Atmospheric Science Dept., Colorado State University, Fort Collins, 33 pp.
- \_\_\_\_\_ and J.D. Mahlman, 1965: Heavy radioactive fallout over the southern United States, November 1962. *J. Geophys. Res.*, Vol. 70, pp. 4501-4520.
- Scorer, R.S., 1949: Theory of waves in the lee of mountains. *Q.J. Roy. Meteor. Soc.*, Vol. 75, pp. 41-56.
- \_\_\_\_\_, 1953: Theory of airflow over mountains: II - The flow over a ridge. *Q.J. Roy. Meteor. Soc.*, Vol. 79, pp. 70-83.
- \_\_\_\_\_, 1954: Theory of airflow over mountains: III - airstream characteristics. *Q.J. Roy. Meteor. Soc.*, Vol. 80, pp. 417-428.
- \_\_\_\_\_, 1967: Causes and consequences of standing waves. In *Proceedings of the Symposium on Mountain Meteorology, 26 June 1967*, Atmospheric Science Tech. Report No. 122, Atmospheric Science Dept., Colorado State University, Fort Collins, pp. 75-101.

Appendix

Photographs of orographically formed cloud formations to the immediate lee of the Colorado Rockies.

---

---

---

---

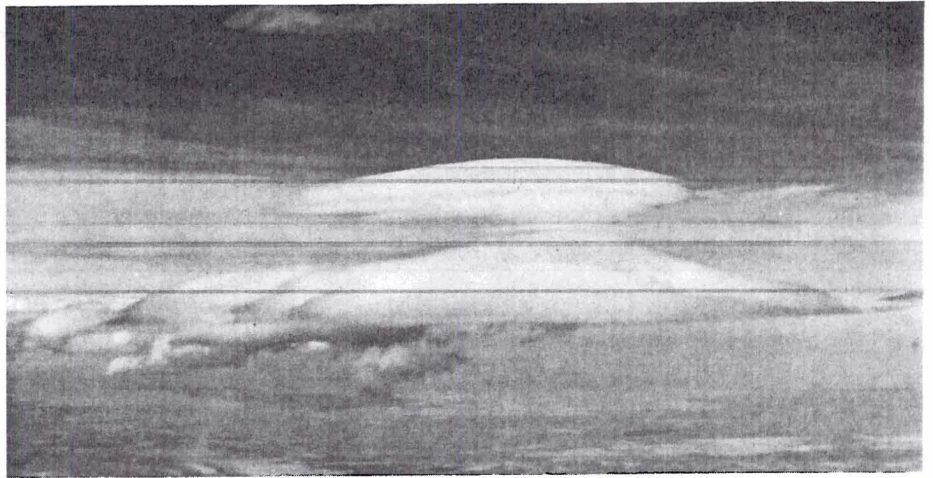


Figure A1. Wave cloud formation taken from The Explorer (10 Oct. 1968) at 6.1 km (20,000 feet).

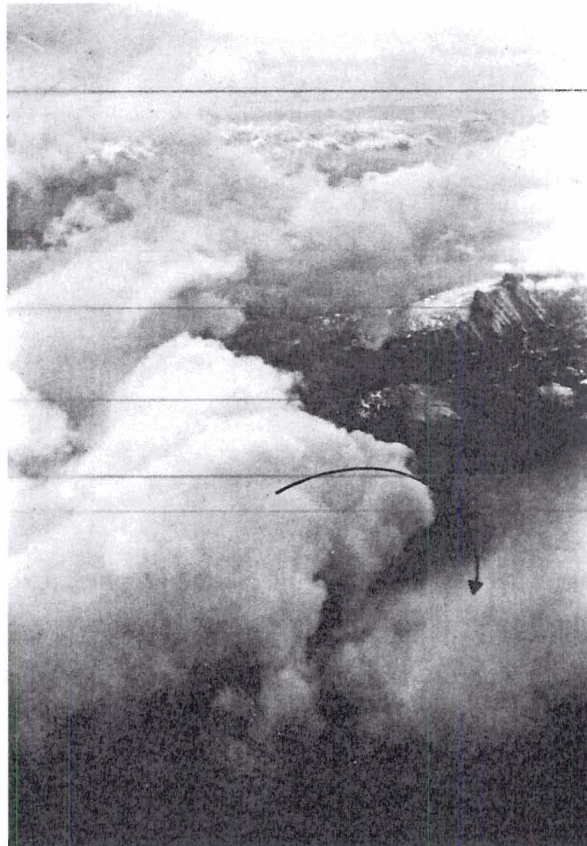


Figure A2. Rotor cloud near Longs Peak, 10 Oct. 1968. (Motion in the rotor is clockwise in this picture - a good theoretical discussion relative rotors is given by *Kuettner* [1959] and *Scorer* [1967]).

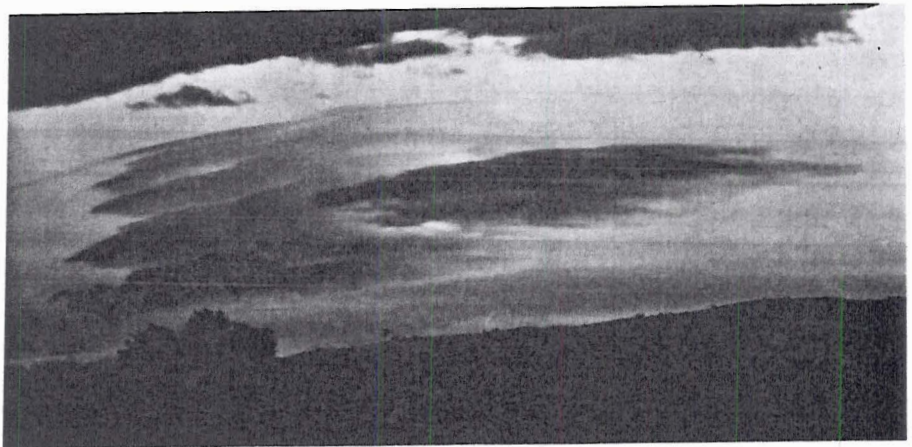


Figure A3. Multi-layer lenticular cloud near Longs Peak, fall 1968 (as the wind blows through, the cloud remains quasi-stationary).

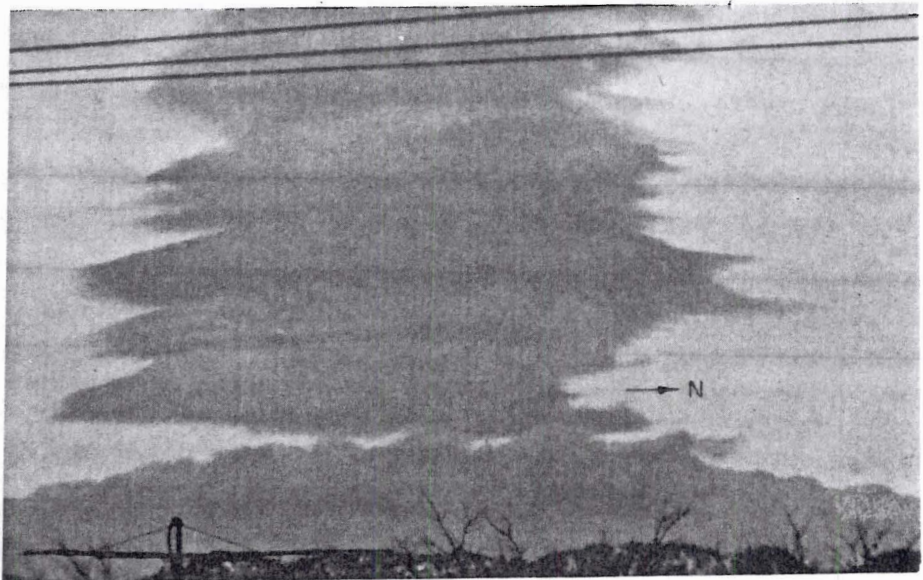


Figure A4. Multi-layer lenticular cloud near Hagues Peak, fall 1968 (see Figure 8 of text). (See comment, Figure A3) (Photographed with 400mm lens.)



Figure A5. (Left) Lee wave over Continental Divide as seen from Estes Park, fall 1968 (viewed to the south). (Note the laminar flow regions.)

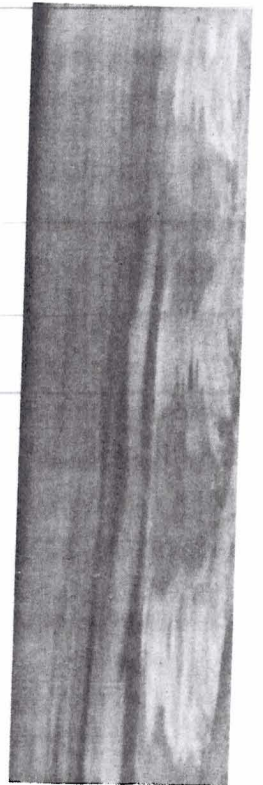


Figure A6. (Below) Mosaic photograph of train of six lee waves taken from The Explorer at 6.1 km (20,000 feet) MSL. (The estimated vertical thickness of the standing waves was 2-3 km.)

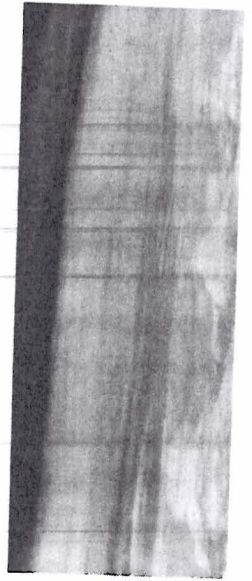






Figure A7a. Billow cloud formations near Continental Divide, January 1969. (A good theoretical discussion of the billow cloud is given by *Scorer* [1967].) (Note: 55mm lens used for this photograph)

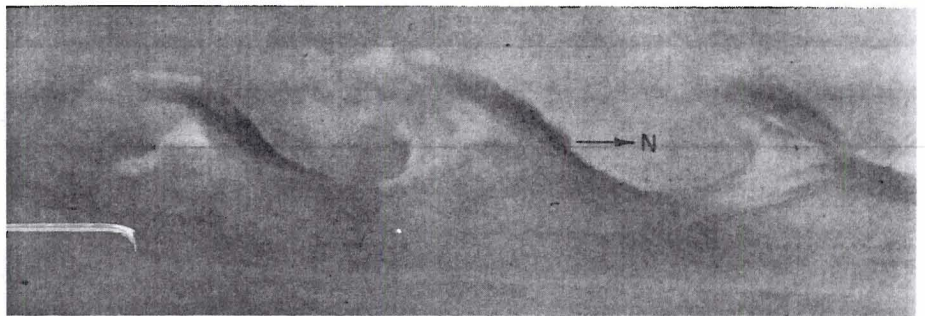


Figure A7b. As Figure A7a except 200mm lens.

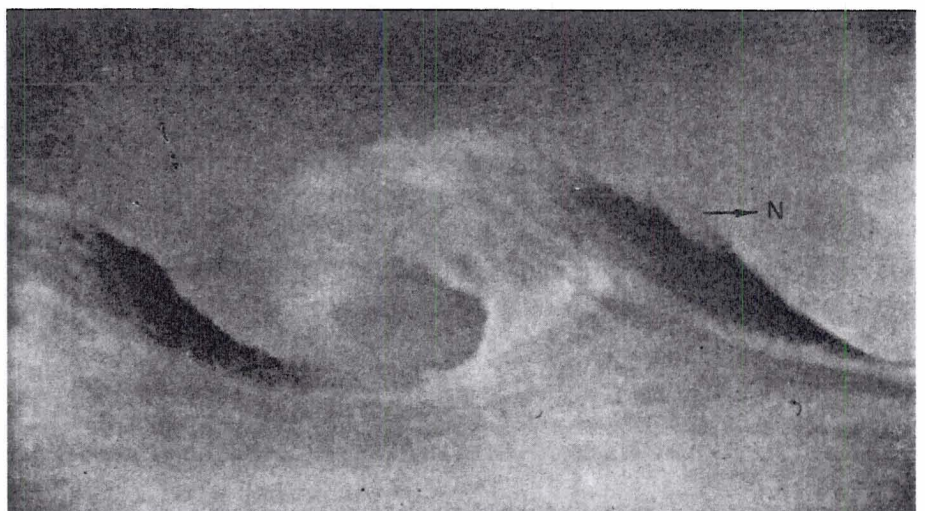


Figure A7c. As Figure A7a except 400mm lens.

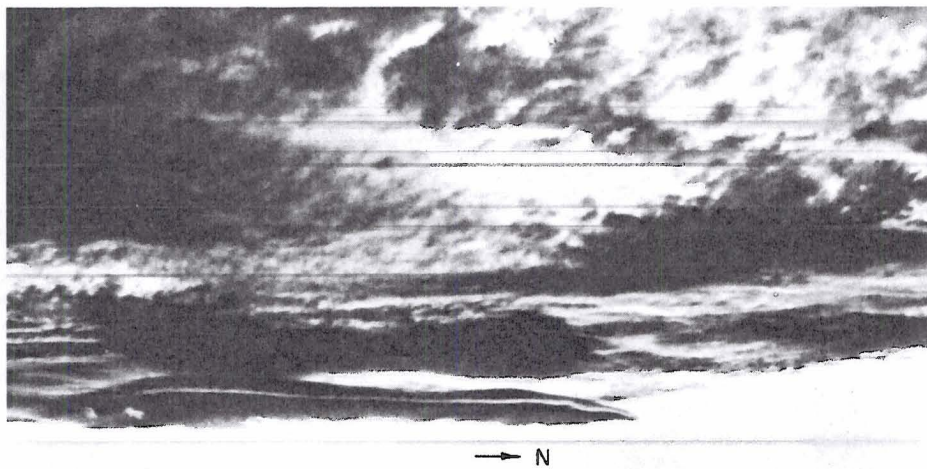


Figure A8a. Wave cloud formation to the lee of the Continental Divide, near Longs Peak, January 1969. (Note the extremely vivid lens shape detail (50mm lens))

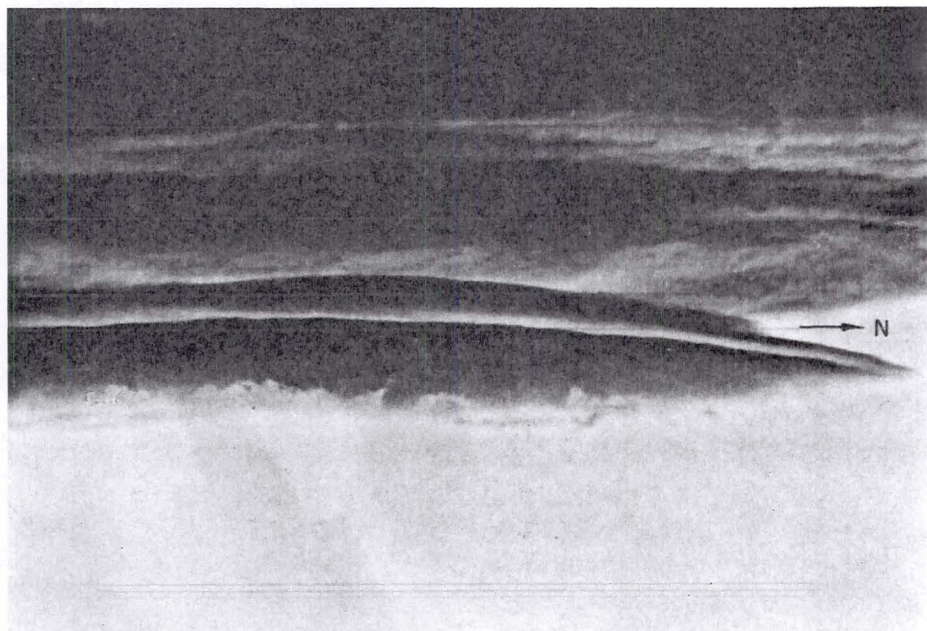


Figure A8b. As Figure A8a except 400mm lens.

RECENT ATMOSPHERIC SCIENCE PAPERS

26. *Studies on Interaction Between Synoptic and Mesoscale Weather Elements in the Tropics. Part I: Some Aspects of Cumulus-Scale Downdrafts*; Herbert Riehl. *Part II: Vorticity Budgets Derived from Caribbean Data*; Robert P. Pearce, Imperial College, London.
27. *A Three-Dimensional Spectral Prediction Equation*. T.J. Simons. Prepared under National Science Foundation Grant No. GA-761. July 1968.
28. *Anisotropy in Reflected Solar Radiation*. Vincent V. Salomonson. Supported by National Aeronautics and Space Administration Grant No. NASr-147. August 1968.
29. *Studies in Low-Order Spectral Systems*. F. Baer. Prepared under National Science Foundation Grant No. GA-761. August 1968.
30. *Contributions to a Meteorology of the Tibetan Highlands*. H. Flohn. Prepared with support under Grant E-10-68G National Environmental Satellite Center, ESSA. August 1968.
31. *Computational Stability and Time Truncation of Coupled Nonlinear Equations with Exact Solutions*. F. Baer and T.J. Simons. Prepared under National Science Foundation Grant No. GA-761. August 1968.
32. *Atmospheric Transport Processes. Part I: Energy Transfers and Transformations*. Elmar R. Reiter. Prepared with support from Contract AT(11-1)-1340, U.S. Atomic Energy Commission. October 1968.
33. *Atmospheric Transport Processes. Part II: Chemical Tracers*. Elmar R. Reiter. Prepared with support from Contract AT(11-1)-1340, U.S. Atomic Energy Commission. January 1969.
34. *A High-Rotation General Circulation Model Experiment with Cyclic Time Changes*. Russell L. Elsberry. Supported by Grants from the Office of Naval Research (Contract N000014-67-A-0299-0003-AA) and the Environmental Science Services Administration (Grant E22-138-67(G)). December 1968.

he "Atmospheric Science Papers" are intended to communicate without delay current research results to the scientific community. They usually contain more background information on data, methodology, and results than would normally be feasible to include in a professional journal. Shorter versions of these papers are usually published in standard scientific literature.

Editorial Office: Head, Department of Atmospheric Science  
Colorado State University  
Fort Collins, Colorado 80521

